



Parametric study for performance optimization of pulse detonation engines
by Hasan Zakaria Rouf

A thesis submitted in partial fulfillment of the requirements for the degree of Master of Science in
Mechanical Engineering
Montana State University
© Copyright by Hasan Zakaria Rouf (2003)

Abstract:

The Pulse Detonation Engine (PDE) has recently drawn significant attention in the aero-propulsion community for its potential advantages in performance and inherent simplicity over current propulsion concepts. It is an unsteady propulsion device based on the detonation mode of combustion. The design and optimization of a PDE propulsion system are complex due to the unsteady nature of the propulsion cycle and the strong coupling of the propulsive flow with the vehicle configuration and the ambient environment. Numerical modeling has a major role in the development of this technology. This research presents a systematic parametric investigation of PDE performance using an unsteady numerical simulation model which is second order accurate in space and first order accurate in time. The numerical modeling was performed using an automated Java based computational fluid dynamics (CFD) software written with modern object-oriented programming technique. One- and two-dimensional transient CFD models were employed in a systematic manner to study the propulsive performance characteristic of the PDE under different operating conditions. Effects of PDE combustor length, fill pressure, initial temperature, ambient conditions, and equivalence ratio were examined through numerical simulations. Both uniform and non-uniform fuel-filling schemes were investigated. Systematic computations were also performed to investigate the effects of nozzle length and nozzle expansion ratio.

This study reveals that the addition of a nozzle to the PDE combustor has the potential for a significant improvement in the PDE performance. The obtained results indicate that the presence of a divergent nozzle enhances the impulse generation rate, whereas the presence of a straight nozzle or a convergent nozzle leads to a slower impulse generation. The cycle time was also found to be considerably affected by the nozzle geometry. It was observed that for very high altitude cruises when the ambient pressure is very low, the presence of a nozzle significantly increases the specific impulse of the PDE. The results suggest that a variable geometry nozzle, capable of adapting with the cycle-time and the ambient conditions, is suitable for PDE performance optimization. This study also confirms that the specific impulse can be considerably increased through mixture control; it was found that the use of a leaner mixture dramatically increases the specific impulse of the PDE.

PARAMETRIC STUDY FOR PERFORMANCE OPTIMIZATION OF PULSE
DETONATION ENGINES

by

Hasan Zakaria Rouf

A thesis submitted in partial fulfillment
of the requirements for the degree

of

Master of Science

in

Mechanical Engineering

MONTANA STATE UNIVERSITY – BOZEMAN
Bozeman, Montana

April 2003

N378
R754


APPROVAL

of a thesis submitted by

Hasan Zakaria Rouf

This thesis has been read by each member of the thesis committee and has been found to be satisfactory regarding content, English usage, format, citations, bibliographic style, and consistency, and is ready for submission to the College of Graduate Studies.

Dr. M. Ruhul Amin



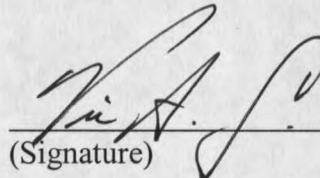
(Signature)

18 April 2003

Date

Approved for the Department of Mechanical and Industrial Engineering

Dr. Vic Cundy



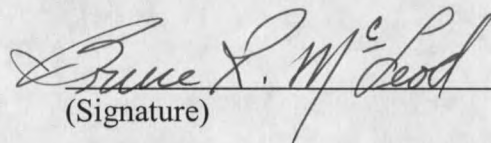
(Signature)

4-18-03

Date

Approved for the College of Graduate Studies

Dr. Bruce McLeod



(Signature)

4-30-03

Date

STATEMENT OF PERMISSION TO USE

In presenting this thesis in partial fulfillment of the requirements for a master's degree at Montana State University – Bozeman, I agree that the library shall make it available to borrowers under rules of the Library.

If I have indicated my intention to copyright this thesis by including a copyright notice page, copying is allowable only for scholarly purposes, consistent with "fair use" as prescribed in the U.S. Copyright Law. Requests for permission for extended quotation from or reproduction of this thesis (paper) in whole or in parts may be granted only by the copyright holder.

Signature Hasan Zakaria Rong

Date April 18, 2003

ACKNOWLEDGEMENTS

I would like to express my sincere gratitude to my adviser, Dr. Ruhul Amin, for his guidance throughout my research. Dr. Amin's continued support and enthusiasm was instrumental to the success of my research. I would like to thank Dr. Alan George and Dr. William Martindale for their dedicated work as committee members.

I am profoundly indebted to Dr. J.-L. Cambier for the original version of the computer code *Café-Vienna* used in the present work and for his guidance and support throughout this research.

I am grateful to the Department of Mechanical and Industrial Engineering for providing me with the financial assistance.

I would like to thank my course instructor Dr. Ladean McKittrick and my fellow graduate students especially Joel, Christopher, Dan, Ezana, Harish, and Jay for their scholarly support.

Finally, I gratefully acknowledge the encouragement and support of my parents, M. Abdur Rouf and Mrs. Lutfun Nahar Rouf, and my brothers, Shahariar and Khaled.

TABLE OF CONTENTS

LIST OF TABLES	vii
LIST OF FIGURES	viii
NOMENCLATURE	xii
ABSTRACT.....	xv
1. INTRODUCTION	1
Operating Principle of a Typical Pulse Detonation Engine.....	3
Background	4
Motivation.....	15
The Scope of the Current Work.....	18
2. BASIC CONCEPTS OF A PULSE DETONATION ENGINE	20
Deflagration and Detonation.....	20
Basic Engine Operation	21
Efficiency of the PDE	23
3. PROBLEM FORMULATION AND NUMERICAL METHODOLOGY	26
Governing Equations	26
Reaction Kinetics	30
Computational Methodology	33
The CFD Model	33
Numerical Procedure	35
4. CODE VALIDATION & GRID SENSITIVITY ANALYSIS.....	37
Code Validation	37
Grid Sensitivity Studies	40
5. RESULTS AND DISCUSSION.....	43
Effects of Tube Length	45
Effects of the Fill Pressure.....	50
Effects of the Initial Temperature.....	53
Effects of Tube Fill Fraction.....	57
Effects of Nozzle Geometry.....	65

Diverging Nozzle	66
Straight Nozzle.....	72
Converging Nozzle	75
Length of Straight Nozzle.....	79
Exit Area of Diverging Nozzle	84
Length of Divergent Nozzle.....	88
Effects of Ambient Pressure	94
Mixture Effects	97
Uniform Mixture.....	97
Non-Uniform Mixture.....	102
6. CONCLUSIONS.....	107
REFERENCES CITED.....	110

LIST OF TABLES

Table	Page
Table 1. Different Grid Resolutions.....	40
Table 2. Input data	53

LIST OF FIGURES

Figure	Page
1. Schematic of a typical air-breathing pulse detonation engine	4
2. Pressure –Volume and Temperature-Entropy cycle Diagram	23
3. Specific impulse compared to the experimental results of Schauer et al. (2001)	39
4. Specific impulse compared to the analytical predictions of Wintenberger et al. (2001).	39
5. Pressure profiles for different grid resolutions	41
6. PDE pressure history for different grid resolutions	42
7. Schematic of a pulse detonation engine	46
8. Instantaneous thrust profile for different tube lengths	47
9. Impulse trace for different tube lengths	48
10. Variation of maximum impulse of a cycle with PDE tube length	49
11. Variation of specific impulse with respect to PDE tube length	49
12. Impulse per unit volume comparison between numerical results and analytical results of Wintenberger et al. (2001), for varying fill pressure.....	51
13. Specific impulse comparison between numerical results and analytical results of Wintenberger et al. (2001), for varying fill pressure	52
14. Impulse per unit volume versus initial temperature for different filling pressures....	55
15. Specific Impulse versus initial temperature for different filling pressures.....	56
16. Schematic of the straight tube PDE with partial tube filling	57
17. Thrust profiles for different tube fill fractions (TFF)	59
18. Impulse profiles for different tube fill fractions	59

LIST OF FIGURES—continued

Figure	Page
19. Impulse versus tube fill fraction	61
20. Specific impulse versus tube fill fraction.....	62
21. Specific impulse versus temperature of air in stratified charge	63
22. Pressure profile at two different times for tube fill fraction 0.6	64
23. Schematic of a divergent nozzle attached with a PDE tube.....	67
24. Effect of divergent nozzle on the thrust.....	68
25. Effect of divergent nozzle on the impulse	69
26. Effect of divergent nozzle on PDE pressure history	71
27. Effect of divergent nozzle on PDE temperature	71
28. Effect of straight nozzle on the thrust.....	73
29. Effect of straight nozzle on the impulse	74
30. Effect of straight nozzle on PDE pressure history	75
31. Schematic of the computed configuration for PDE tube with convergent nozzles of different shapes.....	76
32. Effect of convergent nozzle on the impulse.....	77
33. Effect of convergent nozzle on the thrust	78
34. Impulse traces for different lengths of straight nozzle.....	80
35. Specific impulse versus length of straight nozzle.....	81
36. Instantaneous thrust profile for different lengths of straight nozzle	82
37. Blow-down time (defined as time when P_{pde} drops to 1 atm) versus length of straight nozzle	83

LIST OF FIGURES—continued

Figure	Page
38. Effect of straight nozzle length on PDE temperature	83
39. Thrust profiles for different exit radius of divergent nozzle.....	85
40. Impulse as a function of time for different exit radius of divergent nozzle.....	85
41. Specific impulse as function of expansion ratio of a divergent nozzle.....	87
42. Specific impulse versus expansion ratio: contribution from PDE combustor only.....	87
43. Blow-down time versus expansion ratio.....	88
44. Schematic of the computed configuration for PDE tube with divergent nozzles of different lengths.....	89
45. Specific impulse versus length of divergent nozzle where the nozzle exit area is kept constant.....	91
46. Blow-down time versus length of divergent nozzle where nozzle exit area is kept constant.....	91
47. Schematic of the computed configuration for a PDE tube with divergent nozzles of different lengths where the divergence angle is kept constant	92
48. Specific impulse versus length of divergent nozzle where divergence angle is kept constant.....	93
49. Impulse as a function of time for different ambient pressures.....	95
50. Specific impulse versus ambient pressure for different configurations.....	96
51. Impulse per unit volume varying with equivalence ratio.....	99
52. Specific impulse versus equivalence ratio for uniform filling scheme and using equilibrium model	100

LIST OF FIGURES—continued

Figure	Page
53. Specific impulse versus equivalence ratio for uniform filling scheme and using full chemical kinetics of combustion	101
54. Specific impulse versus equivalence ratio for uniform filling scheme and using full chemical kinetics and equilibrium model	102
55. Specific impulse versus equivalence ratio for non-uniform filling scheme	104
56. Specific impulse versus equivalence ratio for uniform and non-uniform filling scheme and full chemical kinetics of combustion.....	105
57. Impulse per unit volume varying with equivalence ratio.....	106

NOMENCLATURE

<u>Symbol</u>	<u>Description</u>
A	thrust-wall area
A_{exit}	nozzle exit area
A_{tube}	cross-sectional area of PDE tube
C	frequency factor
C_p	specific heat at constant pressure (per unit mass)
C_v	specific heat at constant volume (per unit mass)
E	total energy
E_{int}	internal energy
F	vector of fluxes in x direction
G	vector of fluxes in y direction
I	single cycle impulse
I_{sp}	specific impulse
Imp_{final}	final impulse at the end of a pulse
Imp_{max}	maximum impulse during a single pulse
I_{sp_final}	specific impulse computed from the final impulse at the end of a pulse
I_{sp_max}	specific impulse computed from the maximum impulse during a single pulse
I_v	impulse per unit volume
k	Boltzmann constant

NOMENCLATURE – continued

k_r	reaction rate
L_{pde}	PDE tube length
L_{nozzle}	nozzle length
m_s	molar mass of specie s
\bar{M}	average molar mass
M_{fuel}	fuel mass
N	number of molecules per unit volume
N_s	number density variable of specie s
P	pressure
Q	vector of conserved variables
R	gas constant
R_{pde}	radius of PDE tube
R_{exit}	exit radius of nozzle
S	surface area
t	time
T	absolute temperature
u	mean flow velocity (in x direction)
v	mean flow velocity (in y direction)
V	volume
V_{pde}	PDE combustor volume

NOMENCLATURE – continued

Z_s	electric charge of specie s
β	fit parameter
θ	activation energy
ρ	density
ρ_s	mass density of specie s
γ	ratio of specific heats
$\bar{\gamma}$	adiabatic index for real gas
$\dot{\omega}_s$	rate of production of specie s per unit volume
ν_s	stoichiometric coefficient of specie s
η	cycle efficiency

ABSTRACT

The Pulse Detonation Engine (PDE) has recently drawn significant attention in the aero-propulsion community for its potential advantages in performance and inherent simplicity over current propulsion concepts. It is an unsteady propulsion device based on the detonation mode of combustion. The design and optimization of a PDE propulsion system are complex due to the unsteady nature of the propulsion cycle and the strong coupling of the propulsive flow with the vehicle configuration and the ambient environment. Numerical modeling has a major role in the development of this technology. This research presents a systematic parametric investigation of PDE performance using an unsteady numerical simulation model which is second order accurate in space and first order accurate in time. The numerical modeling was performed using an automated Java based computational fluid dynamics (CFD) software written with modern objected-oriented programming technique. One- and two-dimensional transient CFD models were employed in a systematic manner to study the propulsive performance characteristic of the PDE under different operating conditions. Effects of PDE combustor length, fill pressure, initial temperature, ambient conditions, and equivalence ratio were examined through numerical simulations. Both uniform and non-uniform fuel-filling schemes were investigated. Systematic computations were also performed to investigate the effects of nozzle length and nozzle expansion ratio.

This study reveals that the addition of a nozzle to the PDE combustor has the potential for a significant improvement in the PDE performance. The obtained results indicate that the presence of a divergent nozzle enhances the impulse generation rate, whereas the presence of a straight nozzle or a convergent nozzle leads to a slower impulse generation. The cycle time was also found to be considerably affected by the nozzle geometry. It was observed that for very high altitude cruises when the ambient pressure is very low, the presence of a nozzle significantly increases the specific impulse of the PDE. The results suggest that a variable geometry nozzle, capable of adapting with the cycle-time and the ambient conditions, is suitable for PDE performance optimization. This study also confirms that the specific impulse can be considerably increased through mixture control; it was found that the use of a leaner mixture dramatically increases the specific impulse of the PDE.

CHAPTER 1

INTRODUCTION

The Pulse Detonation Engine (PDE) has recently received considerable interest in the aero-propulsion community due to its potential advantages in performance and inherent simplicity over current propulsion concepts. It is a very promising propulsion concept for aerospace transportation. The PDE uses detonation waves that are initiated at the end of a combustor and propagate through a propellant mixture with a supersonic speed and produce very high pressure and temperature to trigger the chemical reactions. Due to the rapid detonation process, nearly constant volume combustion is achieved, which has a higher thermal efficiency than a traditional constant pressure combustion process [Bussing and Pappas (1994)].

The Pulse Detonation Engine is an unsteady propulsion device. It is based on the detonation mode of combustion, which involves the burning of a reactive gas mixture at the high pressure and high temperature behind a propagating shock wave. The high-pressure combustion products, acting on the thrust plate at the front end of the engine, produce the forward thrust.

The operation of the PDE is distinguished from the operation of the steady-state standard rocket engine or turbojet by its cyclic operation. The PDE is an unsteady propulsion device, which operates in an intermittent manner governed by a cycle frequency. Following Eidelman et al. (1991), one complete detonation cycle is comprised of mixture loading, detonation initiation, detonation propagation, and purging of the

detonation products. Each process is unsteady in nature and interdependent. The interaction and timing of the interdependent processes are crucial for multi-cycle engine efficiency.

The PDE is expected to become the next generation of aerospace propulsion engines. Following Bussing et al. (1997) and Kim (1999), the thermodynamic efficiency of the pulse detonation engine is higher than that of the traditional constant pressure combustion process, standard in conventional aerospace propulsion engines. It is mechanically simple and cost effective. It is suitable for a wide range of flight Mach numbers, regardless of the engine size and shape. Some of the anticipated advantages of the PDE are (a) higher thermodynamic efficiency, (b) higher specific impulse (lower specific fuel consumption), (c) compactness of engine design due to the capability to operate at a very high energy density, (d) very high operating frequency, (e) high combustion chamber pressure, and (f) high thrust per unit weight.

The design and optimization of a PDE propulsion system are complex due to the unsteady nature of the propulsion cycle and the strong coupling of the propulsive flow with vehicle configuration and ambient environment. Numerical modeling and the use of simplified analytical models can play a major role towards the development of this technology. An intensive numerical effort is currently underway in order to quantify the performance characteristics of the pulse detonation engine. This research presents a systematic parametric investigation of the performance of the PDE using an unsteady numerical simulation model, which is second order accurate in space and first order accurate in time. One- and two-dimensional transient CFD models are employed in a

systematic manner to elucidate the propulsive performance characteristics of the PDE over a wide range of operating conditions.

Operating Principle of a Typical Pulse Detonation Engine

The pulse detonation engine operates in a cyclic manner. One complete cycle consists of filling the PDE combustor with unburned propellants, detonation initiation, detonation propagation, and finally exhaust of the combustion products. Figure 1 shows a schematic of a typical air-breathing pulse detonation engine, which consists of a simple straight cylindrical tube. The tube, also called the PDE combustor, is open at one end and closed at the other. At the beginning, fuel and air are introduced in the PDE combustor through the inlet valves. Then the valves are closed and detonation is initiated by electric sparks which in turn produce a large amount of energy near the closed end. After being initiated at the closed end, the detonation wave propagates through the PDE combustor at a supersonic speed. The detonation wave causes enormous rise of pressure and temperature inside the PDE tube which initiates the combustion process. When the detonation wave leaves the PDE tube it is quenched, as there is no fuel outside of the PDE tube. The burned gases are then exhausted, and the momentum of the exhaust gases produces the forward thrust. Detail description of the PDE operation is reported later in Chapter 2.

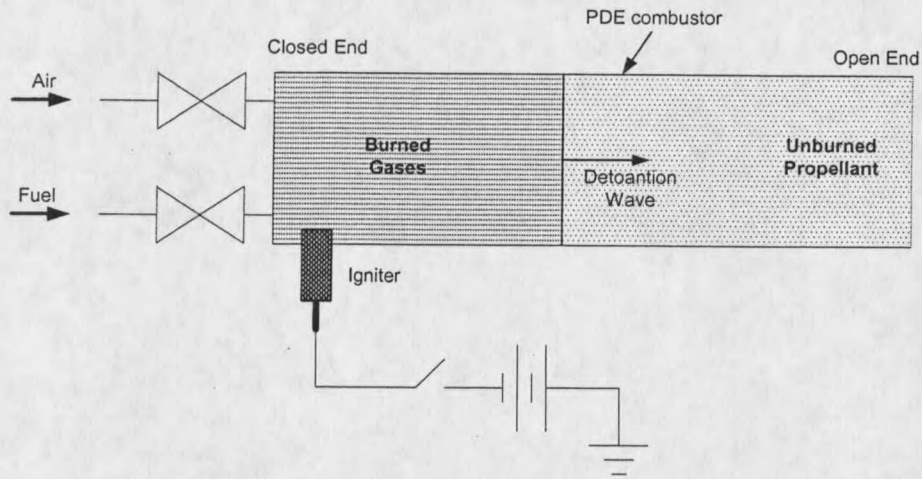


Figure 1. Schematic of a typical air-breathing pulse detonation engine

Background

Eidelman and Yang (1998) reported that Helman et al. (1986) introduced the modern PDE concept in 1986. Subsequently a number of analytical, computational and experimental studies were performed. Performance estimations of the PDE are mostly carried out by the methods of computational fluid dynamics (CFD). The performance estimations by the CFD methods are more accurate than the simplified analytical methods. As reported by Kim (1999), numerical investigations on PDE performance have progressed following the development of computational methods on high-temperature non-equilibrium flows.

Cambier and Adelman (1988) reported a numerical study of a pulse detonation wave engine (PDWE) using quasi one-dimensional computations. The computations were carried out with a shock-capturing total variation diminishing (TVD) algorithm for multiple species and multi-step finite-rate kinetics. The algorithm is second-order

accurate in space. A straight cylindrical tube, with a diverging nozzle connected at the aft end of the tube, was considered. Their results indicated that a pulse detonation wave engine can produce a very high specific impulse (of the order 6500 sec). They predicted cyclic frequency 667 Hz. The predicted value of the specific impulse and the cyclic frequency were higher than the experimental observations. The authors identified that a PDWE could be operated in rocket mode with all the oxidizer supply carried on board. In this mode their predicted specific impulse was around 800 sec, which is higher than conventional rocket engines.

Eidelman et al. (1989) performed two-dimensional simulations of a detonation tube using a second-order Godunov solver on unstructured grids. Their system consisted of a straight cylindrical tube with uniform cross-section with a converging nozzle connected at the aft end of the tube. The detonation was initiated at the open end and it traveled towards the closed end. In case of open end initiation, the pressure developed due to reflection of the wave at the thrust wall is higher than that during a closed end initiation. They concluded that the best performance can be obtained for open-end detonation initiation, i.e. when the detonation wave proceeds upstream to impact on the thrust wall at the closed end of the tube.

Using the same numerical technique, Eidelman et al. (1990) investigated a different configuration with an inlet near the closed end of the PDE tube and no nozzle with the PDE tube. They concluded that for the best performance, the detonation initiation must take place in the vicinity of the exit plane of the chamber resulting in initial propagation of the wave towards the thrust wall. The results indicated that the

internal flow processes (detonation, expansion, intake) are directly coupled with external flow processes (shock formation, stagnation point formation etc).

A detailed description of the basic operations of a PDE was provided by Bussing and Pappas (1994). They described the basic physics associated with the operation of a PDE. The authors concluded that a detonation combustion process is thermally more efficient than traditional constant pressure combustions. They performed some preliminary simulations using the *Mozart* quasi-1D CFD code developed by Dr. J.-L. Cambier. One-dimensional computations of the PDE combustion with both hydrogen-oxygen and hydrogen-air mixtures were performed. Both air-breathing and rocket mode operation of the PDE were discussed. The authors considered closed-end detonation initiation using an energetic initiation region adjacent to the closed end.

In a subsequent study performed by Bussing et al. (1994), a comparison between open- and closed-end initiations was provided. The one-dimensional computations showed an equivalent performance between open-end and closed-end detonation initiation. Equivalent impulse generation and fuel efficiency were observed for both cases. The authors recommended only a diverging nozzle at PDE tube end to fully expand the combustion gases to ambient pressure.

Cambier and Tenger (1997) analyzed the effects of different cycling parameters, fueling strategies, and nozzle geometries on the performance of a PDE. Their results indicated that the presence of a nozzle can significantly affect the performance of a PDE. Five different nozzle shapes were studied; the bell shaped nozzle gave better performance than the shapes with positive curvature. Flow dynamics and phase duration were also

reported to be affected by the presence of a nozzle. They identified that the multi-cycle estimations can be significantly different from single pulse estimations. For their configuration, closed-end ignition initiation gave better performance than open-end initiation. The same result was reported by Bussing et al. (1994). They identified the need of a computational scheme that is capable of isolating the contribution of the detonation initiation energy for multi-cycle operation. Their results indicated that the cyclic frequency can be increased by proper selection of injection pressure.

Ebrahimi(1999) performed one- and two-dimensional transient CFD computations for evaluating operational performance of PDEs with hydrogen-oxygen propellants. The Generalized Propulsion Algorithm with Chemical Kinetics and Two-Phase Flow (GPACT) computer program was applied to perform the simulations of the unsteady processes associated with a PDE operation. A kinetic model using 8 species and 16 reactions was employed. Methods of detonation initiation were examined. Comparisons between open- and closed-end detonation initiation processes were reported. The results indicate that the open-end detonation initiation results in a rapid establishment of the detonation wave within a shorter distance compared to the closed-end detonation initiation. It was observed that the elevated wall temperature stimulates some reactions near the wall in case of multi-cycle studies. However, in the grid sensitivity study the authors got unacceptable results with very fine grids.

Mohanraj et al. (2000) studied multi-cycle performance of a PDE using a quasi one-dimensional model with a single progress variable equation to represent chemical reactions. Closed-end detonation initiation was considered. Results of a parametric study

to investigate the effects of ambient pressure, nozzle, injection pressure, and upstream stagnation pressure were presented. The results indicated that both divergent and convergent-divergent nozzles can improve PDE performance at low ambient pressures. However, at a very low ambient pressure the presence of a divergent nozzle may cause performance deterioration.

Bratkovich et al. (1997) reported an analysis of the PDE cycle. The expansion process of the detonation products was assumed to be isentropic. Based on this assumption the PDE cycle analysis was reduced to the analysis of the Humphrey cycle. The Humphrey cycle is more efficient than the Brayton cycle which is used in conventional rocket engines.

Eidelman and Yang (1998) performed numerical investigations of the pulse detonation engine performance using a Second Order Godunov Method on both structured and unstructured grids. Both fuel-air and fuel-oxygen mixtures were considered as propellant. They indicated that equating the PDE cycle with the Humphrey cycle, as reported by Bratkovich et al. (1997), is an oversimplification that misses the kinetic energy of the detonation products, and does not consider the transient nature of the PDE processes. Their results indicated that the PDE cycle is more efficient than the constant volume cycle. The authors concluded that the PDE cycle can be considered as a valve-less implementation of the constant volume cycle. Their results indicated that a nozzle can significantly increase efficiency of the PDEs.

Zitoun et al. (1999) performed experimental and numerical studies to investigate the propulsive potential of reactive mixtures that use detonative combustion. The

experimental setup consists of a straight cylindrical tube as the PDE. The authors computed the specific performance of a multi-cycle pulse detonation engine for various reactive mixtures based on an empirical formula developed from their experimental data. The results indicated that the pressure level inside a PDE combustor is independent of the length to diameter ratio (l/d). Moreover, almost linear dependence of maximum impulse levels with the length to diameter ratio (l/d) of the PDE was observed. Computational results were obtained by employing a numerical algorithm which is based on the method of the flux-corrected transport (FCT) technique. The experimental and numerical results were in good agreement. The results indicated that the specific performance is independent of the size of the combustion chamber.

Cooper et al. (2001) carried out direct impulse measurements for detonations in a tube, closed at one end and open at the other end, by using a ballistic pendulum arrangement. The results showed a satisfactory agreement with the analytical results reported by the Wintenberger et al. (2001). The effects of various exit treatments on the performance of the PDE were examined. The authors observed that a diverging nozzle had a minor effect on the specific performance and concluded that a straight extension is much more effective than the diverging nozzle in increasing the specific performance. The results suggested an increase in the specific performance if the nozzle length is increased.

Schauer et al. (2001) performed an experimental study to investigate the PDE performance using hydrogen-air fuel. In their experiment the PDE was a cylindrical tube uniformly filled with a hydrogen-air propellant mixture and operated at the cycle rate of

16Hz. Their results indicated that the thrust increases linearly with the frequency. The measured detonation wave speed for stoichiometric hydrogen-air mixture was in excellent agreement with the results of Soloukin (1963). The numerical results in the current research were compared with the experimental results of Schauer et al.

Although analytical methods provide approximate solutions, sometimes they are more suitable for a better understanding of PDE performance. Wintenberger et al. (2001) developed an analytical model for the impulse of a single-cycle pulse detonation engine. The PDE was modeled as a straight tube with a constant cross section; one end of the tube was open and the other end was closed. The results predicted by this model showed satisfactory agreement with the experimental results of Schauer et al. (2001). The specific performances for a wide range of fuel-oxygen-nitrogen mixtures were computed. Effects of equivalence ratio, initial chamber pressure, initial chamber temperature, and nitrogen dilution were investigated. The authors reported that the specific impulse is nearly independent of initial pressure and temperature. The results of Wintenberger et al. (2001) were about 20% lower than the results reported by Zitoun et al. (1999). For stoichiometric hydrogen-air mixture the specific impulse predicted by the analytical model is 4335 sec. The numerical results in the current work were compared with the analytical results of Wintenberger et al.

Endo and Fujiwara (2002) estimated the PDE performance analytically by developing a simple model. It was modeled as a straight tube with a constant cross-section; one end of the tube was open and the other end was closed, and a detonation was initiated at the closed end. Viscous effect and thermal conduction were neglected. They

estimated pressure on the thrust wall as a function of time. However, no validation of the analytical model was reported.

Kailasanath and Pantik (2000) performed transient CFD computations for evaluating operational performance of PDEs with hydrogen-oxygen propellants. One major objective of this research was to explore the possible reasons for the differences between various performance predictions. They solved compressible, transient conservation equations for momentum, density, total energy, and number densities of species. A comprehensive kinetic model using 8 species and 48 reactions was employed. In this study the system consisted of a straight cylindrical tube with uniform cross-section, which was modeled with a one-dimensional grid. The authors identified that one dimensional simulations could not model fuel-air mixing properly. Therefore, it was assumed that the detonation tube was filled with a premixed stoichiometric hydrogen-air mixture. A range of values from 4850 sec to 7930 sec (for different pressure relaxation rates) as the specific impulse for a stoichiometric hydrogen-air mixture was obtained. A key observation of this study is that the choice of initial conditions and boundary conditions may significantly contribute to the overall estimated performance. The results of the study suggested that a higher performance can be obtained if the pressure at the end of the tube gradually relaxes to the ambient value.

Li and Kailasanath (2001) performed two-dimensional, transient numerical simulations to study the flow development in a 1350 mm tube. Conservation equations for mass, momentum, energy, and individual species were solved to analyze the flow field inside a PDE tube. All the diffusive transport processes, like thermal diffusion, molecular

diffusion, heat conduction, viscosity, and radiation heat transfer inside the flow field, were neglected. However, it was suggested that for multi-cycle operation the effects of heat transfer through the tube wall are important. Therefore, the effects of diffusive transport processes should be considered. The study was focused on the overall flow development inside a PDE tube. The effects of partial tube fill on the pressure history were also reported. It was concluded that for partial tube filling cases the expansion waves, generated at interface between the reactive propellant mixture and the non-reactive air, can significantly affect the pressure evolution and thrust production. An ethylene-air mixture was found more beneficial than an ethylene-oxygen mixture. The results of this research were confirmed qualitatively by experimental results of Sanders et al. (2000) and Jenkins et al. (2000).

Cambier (1999) presented the results of a numerical study of the performance of a generic pulse detonation rocket engine (PDRE) using the *Mozart* Computational Fluid Dynamics code. Computational methods for dealing with the very high chemical stiffness of high-pressure detonations were presented. A comparison between two-dimensional and quasi-one-dimensional simulations was provided. Nozzle performance was reported to be affected by the ambient pressure. Convergent-divergent nozzles with various throat diameters were examined. The results indicated that the cases with larger throat diameters provide much higher thrusts. It was concluded that the thrust and impulse can be estimated on large time scale by an exponential law. The authors identified the need of evaluating the performance in multi-cycle environment and extending the analysis to a realistic environment where the performance is a function of the ambient pressure.

Sterling et al. (1995) analyzed the performance of an air-breathing pulse detonation wave engine (PDWE) over a wide range of Mach numbers. A computational technique to simulate the unsteady operation of a PDWE was presented. One-dimensional numerical simulations were performed to examine the performance of a PDWE operating for multiple cycles. In the analysis the inlet loss and the diffraction of the shock wave at the combustor exit were neglected (by assuming constant pressure boundary condition at the exit) and ideal detonation initiation was assumed. The authors identified that by using controlled gas-dynamics waves the engine can be configured to provide engine aspiration and charge compression. A specific impulse of 5151 sec for a hydrogen-air system was reported.

Kentfield (2000) presented a simple analytical approach to estimate the idealized performance of an air-breathing, hydrocarbon fueled PDE. In this research the system consisted of a straight cylindrical tube with uniform cross-sectional area. Instantaneous flow cut-off valves were assumed to be located at the ends of the detonation tube. A constant volume combustion process was assumed to model the chemical reactions with in the PDE tube. It was concluded that the PDE performance increases with flight Mach number. Another key observation from this study is that initial charge non-uniformities have negligible effect on PDE performance during static operation.

Kim (1999) reported a numerical model to simulate the time-dependent combustion process in a PDE. An inviscid, two-dimensional numerical scheme coupled to the detailed reaction kinetics of combustion was employed. The governing conservation equations were first discretized using a finite volume algorithm, and a time

accurate solution was then obtained by using the Runge-Kutta integration technique. The results of this study were in good agreement with theoretical Chapman-Jouguet data. Different detonation initiation mechanisms were thoroughly examined and the properties of a fully developed detonation wave were found to be independent of the detonation initiation mechanism. A series of shock-induced detonation experiments were performed with a stoichiometric hydrogen-air mixture. The experimental and numerical results agreed well. The numerical results confirmed the postulate that the properties of a fully developed detonation wave are independent of the system geometry whenever the initial conditions and the composition of the fuel-air mixture are the same.

Povinelli and Lee (2001) investigated the effects of flight Mach number on the relative performance of PDE and gas turbine engines. The effects of compression on the inlet temperature and the subsequent sensible heat release were also examined. The results indicated a significant performance benefit during static operation over the gas turbine engine with compression ratio less than 4. They identified that the reduction of sensible heat release due to dissociation of reacting species causes a decrease in the PDE performance. The authors indicated that the PDE may be more suitable for combined cycle applications.

Ebrahimi et al. (2002) presented three different levels of analysis to investigate the performance characteristics of a PDE. The results using the three different models (zero-dimensional, one-dimensional, and two-dimensional) mutually supported each other and provided a better understanding of system performance. It was observed that at vacuum conditions the performance of a PDE is similar to that of a rocket engine and at finite

backpressures, when the pressure inside the PDE is equal to that in the rocket, the rocket gives better performance than the PDE.

Currently, extensive research is being done at The University of California at Los Angeles guided by Dr. A. R. Karagozian. Mathematical and numerical models have been developed. The research is focused on higher order numerical simulations of the generic PDE configuration with simplified chemical reaction kinetics, so that rapid and straightforward estimates of engine performance can be obtained. Both one- and two-dimensional simulations of the high speed reactive flow phenomena are performed and compared to determine the applicability of one-dimensional simulations for performance characterization. Characteristic engine performance parameters and engine noise estimates within and external to the detonation tube are being investigated.

Motivation

The design and optimization of a PDE propulsion system are difficult, due to the unsteady nature of the propulsion cycle. Numerical modeling can play a significant role towards the development of this technology. A number of computational, analytical and experimental studies were performed to estimate the performance of the PDE. However, the concept of PDE suffers from lack of systematic numerical, experimental, and theoretical studies. As reported by Kaliasanath et al. (1999), there are some disagreements between different performance predictions. For example, the predictions of the specific impulse for a hydrogen-air mixture, reported by different researchers, significantly varied. Sterling et al. (1997) predicted an average value of 5151 sec as the specific impulse for a

for a stoichiometric hydrogen-air mixture. Whereas, for the same mixture Bussing et al. (1997) obtained a range of values of 7500 – 8000 sec and Winterber et al. (2001) estimated a value of 4335 sec. Meanwhile, based on experimental results Schauer et al. (2001) reported a specific impulse of 4024 sec for a hydrogen-air system.

A nozzle may significantly affect the performance of a PDE. The optimal PDE nozzle design has yet to be developed. Eidelman and Yang (1998) reported that the addition of a diverging nozzle with a PDE tube can significantly improve the PDE performance. In contrast, based on experimental investigations, Cooper et al. (2001) reported that addition of a diverging nozzle has negligible effect on the PDE performance. Mohanraj et al. (2000) reported that the effect of a diverging nozzle is detrimental at around 1 atm ambient pressure. On the other hand, the results of Eidelman et al. (1998) indicated that at 1 atm. ambient pressure the presence of a divergent nozzle can improve the PDE performance.

Research varies in terms of conclusions regarding open-end and closed-end detonation initiation. There seems to be two schools of thoughts regarding the location of the igniter. In the numerical investigation performed by Cambier and Tenger (1999), the open-end detonation initiation gave better performance than the closed-end initiation. On the other hand, Eidelman et al. (1989) identified the closed-end initiation process to be better than the open-end initiation process. The results of the computational study performed by Bussing et al. (1994) indicated that neither initiation scheme offered a clear performance advantage. As discussed by Kailasanath et al. (1999), the disagreements between different studies could be due to a range of factors, for instance

the geometry of the specific system, boundary conditions, initial conditions, model assumptions, detonation initiation mechanisms etc.

Although nozzles can significantly affect the performance of a PDE, the requirements for the optimal nozzle are not well understood. Only few investigations have been performed on different nozzle geometries. Therefore, it is important to systematically investigate the nozzle effects on PDE performance. For practical implementation of a PDE, it is very important to simulate the performance of a PDE at different altitudes and ambient pressures. However, only a few studies have been aimed at the effects of the ambient condition on the PDE performance. It is not necessarily advantageous to have a stoichiometric propellant mixture over the entire PDE combustor; the specific fuel consumption can be considerably reduced by an optimum fueling strategy. Sufficient information is not available regarding different fueling schemes. Only a few investigations have been done to observe the effects of initial conditions.

Although numerical analysis of the PDE performance dates back almost two decades [Kalaisanath et al. (1999)], there is a lack of systematic and balanced numerical studies. Additional studies are required to establish the role and performance of a PDE in aerospace applications. To get a better and clearer understanding of PDE operational characteristics, a systematic evaluation of the PDE performance is necessary. The primary objective of this research was to elucidate the propulsive performance characteristics of the PDE over a wide range of operating conditions. The results of a systematic numerical investigation of the PDE performance characteristics have been presented here. PDE performance characteristics were studied over a wide range of operating conditions. The

study was performed with an automated Java based CFD software designed with modern object oriented programming techniques. The level of grid resolution and modeling complexity can be varied for each engine component for maximum flexibility and accuracy. One-dimensional and two-dimensional unsteady CFD computations were carried out to get realistic approximations of the unsteady processes of the PDE operation. The numerical scheme used here is second-order accurate in space, total variation diminishing (TVD), and first order accurate in time. Details of this numerical scheme are discussed later.

The Scope of the Current Work

The objective of the work is to utilize Java based automated object-oriented software to perform the parametric investigation for performance optimization of the PDE. The CFD software *Cafe-Vienna*, developed by Dr. J.-L. Cambier, is designed with modern object-oriented programming techniques and implements procedures for automatic cycling. One-dimensional and two-dimensional transient CFD computations were employed to estimate the performance of the PDE. The focus of the study is directed at assessing the overall PDE performance characteristics in a wide range of operating conditions. A systematic study of the performance characteristics of a generic PDE was performed.

The present model is validated by comparing the calculated specific impulse and impulse per unit volume with experimental and analytical results. Computational grid sensitivity was investigated to set the background for the study. Pressure scaling and

length scaling were performed. For different conditions of single cycle operation, specific impulse and impulse per unit volume, impulse history, and thrust history were computed and presented.

Computations were performed to investigate the effects of initial temperature, initial pressure, ambient condition, and equivalence ratio. Both uniform and non-uniform fuel filling schemes were investigated. Computations were performed to estimate effects of air temperature in the non-combustion section of the PDE tube in case of partial tube filling. The PDE performance for different ambient pressures was computed. Effects of different nozzle geometries (convergent nozzle, divergent nozzle, straight nozzle, and convergent-divergent nozzle) were studied. Systematic computations were performed to investigate the effects of nozzle length and nozzle expansion ratio.

CHAPTER 2

BASIC CONCEPTS OF A PULSE DETONATION ENGINE

Deflagration and Detonation

Deflagration and detonation are two different modes of combustion in which waves can be propagated in the form of a chemical reaction in an explosive gas mixture. Following Bussing et al. (1994) and Kim (1999), deflagration is a combustion wave that propagates at a subsonic speed. In this mode of combustion process, the chemical reaction propagates at relatively low flame speed of the order of one meter per second. Due to a small decrease in pressure in this mode of combustion, the process can be modeled as a constant pressure process. The laminar or turbulent molecular diffusion of the gas mixture has a significant role in governing the propagation of the detonation wave. This type of combustion process leads to a net decrease of pressure and fluid density.

Detonation is a combustion wave propagating at a supersonic speed. This is a very energetic and violent phenomenon and results in extremely large increases in pressure and temperature. Following Zeldovich (1960) and Bussing et al. (1994), a detonative combustion process can be characterized by a very rapid propagation of explosive chemical reactions. Due to the high speed, this mode of combustion can be modeled as a constant volume process. Unlike the deflagration process, heat conduction and molecular diffusion have a negligible contribution to a detonation process. Energy transfer is mainly

governed by the mass flow in a strong compression wave. A detonative combustion process results in an increase in both the pressure and the fluid density.

A detonation wave can be approximated as a strong shock. It can be considered as a discontinuity in the gas flow where heat addition occurs. When the detonation front propagates into the unburned gas mixture in the form of a strong shock at a supersonic speed, there is an enormous rise of pressure and temperature in the gas mixture. The temperature is increased by the compression due to the strong shock. This very high pressure and temperature initiate chemical reactions which proceed violently and give off heat at an explosive rate. The moving shock gets energized by the energy released in the chemical reactions. Eventually a self-sustaining detonation wave is formed. The analysis of a detonation process is based on the equations of conservation of mass, momentum and energy, the equation of state, and chemical kinetics of combustion. [Zeldovich (1960), Kim (1999)].

Basic Engine Operation

The Pulse Detonation Engine is an unsteady propulsion device, which operates in a cyclic manner. The PDE cycle can be described according to the fundamental processes that occur during a cycle. Following Eidelamn et al. (1991) and Bussing et al. (1994), one complete detonation cycle consists of the following processes:

1. Filling of the PDE tube with propellant mixture
2. Detonation initiation
3. Detonation propagation along the tube

4. Exhaust of the detonation products to the atmosphere

These processes are interdependent, and the engine efficiency depends on the timing and interactions between these interdependent processes. The total time required to complete all the processes of a detonation cycle is called the cycle time, and the inverse of the cycle time is called the cyclic frequency.

The PDE tube, closed at the left end and open at the right end, is initially filled with a combustible gas mixture. To start the detonation process a detonation initiation zone is set adjacent to the closed end of the PDE tube. Pressure and temperature in that small zone are set sufficiently high to initiate the detonation. After being initiated at the closed end, the detonation wave propagates through the PDE tube. The strong shock from the detonation propagates at a few thousands meters per second relative to the unburned propulsion mixture. Very high pressure and temperature are developed due to the compression by the shock wave; this triggers the combustion process. Energy released from the combustion supports the detonation wave to travel and eventually a self-sustained detonation wave is formed.

When the detonation wave leaves the PDE tube, rarefaction waves are generated at the open end due to the pressure difference at the tube-exit. The rarefaction waves proceed towards the closed end of the combustor and expel the combustion products, thereby, thrust is produced. Intake of fresh combustible mixture begins after chamber pressure falls up to refill level.

Efficiency of the PDE

In the deflagration mode of combustion, the flame propagates at a subsonic speed. Due to small amount of pressure drop, this process can be approximated as a constant pressure process. A constant pressure process can be modeled as a Brayton cycle. Following Bussing et al. (1994) and Bratkovich et al. (1997), in the detonation mode of combustion process, the combustion wave propagates at a supersonic speed, which results in a very rapid propagation of explosive chemical reactions. Due to the high speed, this process can be approximated as a constant volume process, which can be modeled as a Humphrey cycle. Pressure-Volume and Temperature-Entropy cycle diagram for both the Brayton cycle and the Humphrey cycle are shown in Figure 2.

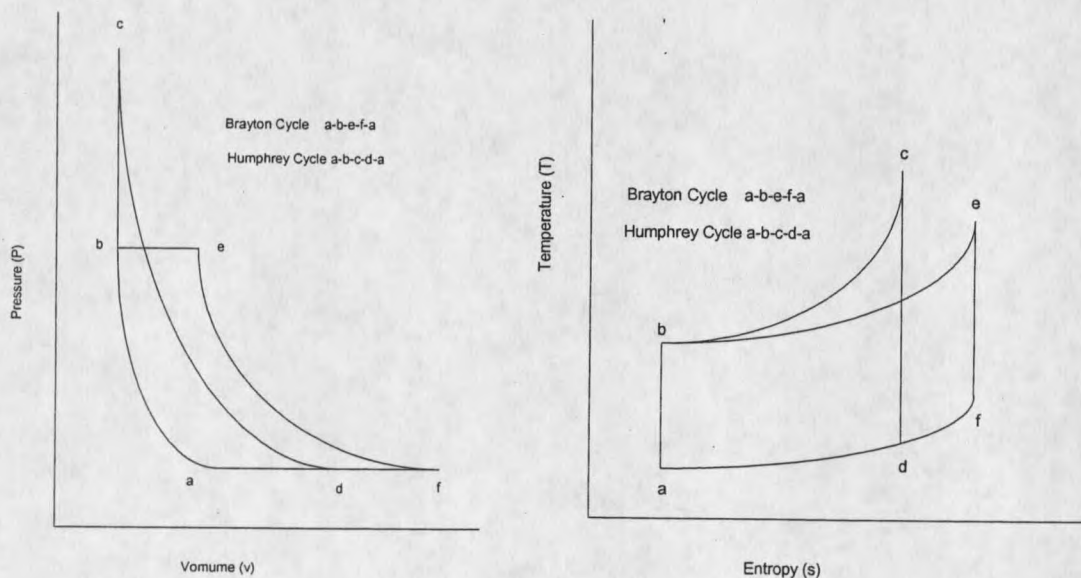


Figure 2. Pressure -Volume and Temperature-Entropy cycle Diagram

The Humphrey cycle is comprised of two isentropic processes (a-b, c-d), one constant pressure process (d-a) and one constant volume process (b-c). On the other hand, the Brayton cycle is comprised of two isentropic processes (a-b, e-f), and two constant pressure processes (b-e, f-a). The main difference between the two cycles is that the constant pressure combustion process (b-e) of the Brayton cycle is replaced by a constant volume heat addition process (b-c) in the Humphrey cycle.

The efficiency of a cycle is defined as the ratio of the work output and the heat energy input. The efficiency of the Brayton cycle is given by

$$\eta_{Brayton} = 1 - \frac{T_a}{T_b} \quad (1)$$

The Brayton cycle efficiency is a function of the ratio of temperatures before and after the isentropic compression (or the isentropic expansion) process. In contrast, the Humphrey cycle efficiency depends on the temperature change due to the isentropic compression (a-b), the temperature change due to the constant volume combustion (b-c), and the ratio of specific heats. The efficiency of the Humphrey cycle is given by

$$\eta_{Humphrey} = 1 - \gamma \frac{T_a}{T_b} \left[\frac{\left(\frac{T_c}{T_b} \right)^{\frac{1}{\gamma}} - 1}{\frac{T_c}{T_b} - 1} \right] \quad (2)$$

The difference between the efficiency of the Humphrey cycle and the Brayton cycle is given as:

$$\eta_{Humphrey} - \eta_{Brayton} = \frac{T_a}{T_b} \left\{ 1 - \gamma \left[\frac{\left(\frac{T_c}{T_b} \right)^{\frac{1}{\gamma}} - 1}{\frac{T_c}{T_b} - 1} \right] \right\} \quad (3)$$

The above expression can be written as,

$$\eta_{Humphrey} - \eta_{Brayton} = \frac{T_a}{T_b} \{1 - \gamma D\} \quad (4)$$

$$\text{where, } D = \left[\frac{\left(\frac{T_c}{T_b} \right)^{\frac{1}{\gamma}} - 1}{\frac{T_c}{T_b} - 1} \right] \quad (5)$$

The value of the expression γD is always less than 1 for any value of γ greater than 1. For a typical detonation process γD is always less than 1. Therefore, the efficiency of the Humphrey cycle is greater than the efficiency of the Brayton cycle. In other words, a constant volume detonation combustion process offers a higher thermal efficiency than a traditional constant pressure deflagration combustion process.

The detonative combustion process of a PDE can be approximated as a constant volume process. Therefore, the PDE combustion process is expected to offer a higher thermal efficiency than a constant pressure combustion process which is typical in conventional rocket engines.

CHAPTER 3

PROBLEM FORMULATION AND NUMERICAL METHODOLOGY

Governing Equations

The following assumptions were made in the formulation of the transient combustion process in a pulse detonation engine:

1. No species diffusion.
2. No heat conduction.
3. Heat flow due to density gradient is neglected.
4. Bulk viscosity is neglected.
5. Diffusion due to pressure gradient is ignored.
6. Heat capacities are a function of temperature.
7. Thermal equilibrium.
8. Viscous dissipation and viscous work are neglected.
9. No body forces.

The time-dependent conservation equations governing the dynamics of the inviscid, non-heat conducting, reacting gas flow, are being solved. The fundamental set of governing equations for the system is:

$$\text{Conservation of Mass:} \quad \frac{\partial \rho}{\partial t} + \frac{\partial(\rho u)}{\partial x} = 0 \quad (6)$$

$$\text{Conservation of momentum:} \quad \frac{\partial(\rho u)}{\partial t} + \frac{\partial(\rho u^2 + P)}{\partial x} = 0 \quad (7)$$

Conservation of Energy:
$$\frac{\partial E}{\partial t} + \frac{\partial(uE + uP)}{\partial x} = 0 \quad (8)$$

Here ρ , ρu and E are the densities of conserved variables, u is the mean flow velocity and P is the gas pressure. The energy in (8) is the total energy, i.e. the sum of kinetic and internal (thermal) energy: $E = \frac{1}{2} \rho u^2 + E_{\text{int}}$. The latter can be simply expressed for an ideal gas as:

$$E_{\text{int}} = \rho C_v T = \frac{P}{\gamma - 1} \quad (9)$$

where C_v is the specific heat at constant volume (per unit mass), and γ is the adiabatic index, i.e. the ratio of specific heats (constant pressure over constant volume): $\gamma = C_p / C_v$.

The specific heats are also related by: $C_p - C_v = R / \bar{M}$, where R is the gas constant in $\text{J.mole}^{-1}.\text{K}^{-1}$ and \bar{M} is the average molar mass (in kg.mole^{-1}) of the gas. Note that here the specific heats have MKS units of $\text{J.kg}^{-1}.\text{K}^{-1}$. Equation (9) relates the pressure to the thermal/internal energy, and is a formulation of the "Equation of State" (EOS) of the system. Another formulation that is always valid is:

$$P = NkT = \rho \left(\frac{R}{\bar{M}} \right) T \quad (10)$$

where k is the Boltzmann constant and N is the total number of molecules per unit volume. For real gases, the specific heats and the adiabatic index are function of temperature. In that case, the internal energy is more accurately described as:

$$E_{\text{int}} = \rho \int_0^T C_v(T) dT \equiv \frac{P}{\bar{\gamma} - 1} \quad (11)$$

Note that by definition the internal energy is zero at $T=0$; this implies that the internal energy described here does not include any potential energy, such as chemical energy of formation. Equation (11) still describes an EOS for the system, along with the definition of an effective adiabatic index $\bar{\gamma}$. Since the conservation equation (8) applies to the total energy E , it is also appropriate to rewrite the EOS as follows:

$$P = (\bar{\gamma} - 1) \left(E - \frac{1}{2} \rho u^2 \right) \quad (12)$$

This form will be used in the numerical method that solves for the conservation equations. One can describe here the general procedure for computing the thermodynamic state of the gas. Given a solution of the conservation equations (6-8), one can obtain at any time the updated values of $\rho, \rho u, E$: let us denote these values at time level (n) by: $\rho^n, (\rho u)^n, E^n$. The temperature at that time level can be obtained by solving for the integral equation:

$$\frac{E^n}{\rho^n} - \frac{1}{2} \left(\frac{(\rho u)^n}{\rho^n} \right)^2 = \int_0^{T^n} C_v dT \quad (13)$$

Once T^n is known, the pressure can be computed according to (10), and the effective $\bar{\gamma}$ is obtained from (12). Knowing all flow variables (conservative and primitive) at time level (n), one can then compute the fluxes and from (6-8), the conserved variables at the next time level ($n+1$).

It is assumed throughout this study that the flow is inviscid, so there is no shear force and the viscosity of the fluid is zero. Neglecting the viscous and the thermal terms, the conservation equations for inviscid flow (6-8) are obtained. Note that the formulation

(6-8) is valid for a one-dimensional problem. More generally, the conservative system can be written as:

$$\frac{\partial \mathbf{Q}}{\partial t} + \vec{\nabla} \mathbf{F} = 0 \quad (14)$$

where \mathbf{Q} and \mathbf{F} are vectors in the variable space, i.e. each component of \mathbf{Q} is a conserved variable and each component of \mathbf{F} is a flux. In one space dimension:

$$\mathbf{Q} = \begin{Bmatrix} \rho \\ \rho u \\ E \end{Bmatrix}, \quad \mathbf{F} = \begin{Bmatrix} \rho u \\ \rho u^2 + P \\ u(E + P) \end{Bmatrix} \quad (15)$$

In two dimensions, the system of conservation includes one additional equation since there are now two components of the momentum density, and one more flux \mathbf{G} (the flux components are traditionally denoted \mathbf{F}, \mathbf{G} in Computational Fluid Dynamics (CFD)).

Considering also the chemical source terms, for two-dimensional cases the conservation equations can be written as

$$\frac{\partial \mathbf{Q}}{\partial t} + \frac{\partial \mathbf{F}}{\partial x} + \frac{\partial \mathbf{G}}{\partial y} = S \quad (16)$$

where the right-hand-side represents the chemical source terms. In two space dimensions the vector of conserved variables and the flux vectors are then given by,

$$\mathbf{Q} = \begin{Bmatrix} \rho \\ \rho u \\ \rho v \\ E \end{Bmatrix}, \quad \mathbf{F} = \begin{Bmatrix} \rho u \\ \rho u^2 + P \\ \rho uv \\ u(E + P) \end{Bmatrix}, \quad \mathbf{G} = \begin{Bmatrix} \rho v \\ \rho uv \\ \rho v^2 + P \\ v(E + P) \end{Bmatrix} \quad (17)$$

For reacting flows, the mass conservation equation is generalized to multiple species. For multiple species (in two dimensions) the vector of conserved variables and the flux vectors are then given by ,

$$\mathbf{Q} = \begin{Bmatrix} \rho_1 \\ \cdot \\ \cdot \\ \cdot \\ \rho_n \\ \rho u \\ \rho v \\ E \end{Bmatrix}, \quad \mathbf{F} = \begin{Bmatrix} \rho_1 u_1 \\ \cdot \\ \cdot \\ \cdot \\ \rho_n u_n \\ \rho u^2 + P \\ \rho uv \\ u(P + E) \end{Bmatrix}, \quad \mathbf{G} = \begin{Bmatrix} \rho_1 v_1 \\ \cdot \\ \cdot \\ \cdot \\ \rho_n v_n \\ \rho uv \\ \rho v^2 + P \\ v(P + E) \end{Bmatrix} \quad (18)$$

In this equation, n is the total number of species. The first n rows represent species continuity equations. The next two rows represent momentum conservation equations and the final row represents the energy conservation equation.

The above set of equations, representing the conservation laws for a compressible flow, for which the effects of body forces, viscous stresses and heat flux are neglected, are the governing equations used to simulate the inviscid propagation of detonation with irreversible chemical reaction.

Reaction Kinetics

The physical and chemical effects of combustion are modeled by solving the chemical kinetics equations. Consider the general form of the conservation equations for the mass densities of chemical species (index s):

$$\frac{\partial \rho_s}{\partial t} + \vec{\nabla} \cdot (\vec{u} \rho_s) = m_s \dot{\omega}_s \quad (19)$$

where \bar{u} is of course the mean flow velocity, m_s is the molar mass and $\dot{\omega}_s$ is the rate of production of species s per unit volume. Summation over all species yields:

$$\sum_s \left[\frac{\partial \rho_s}{\partial t} + \bar{\nabla} \cdot (\bar{u} \rho_s) \right] = \frac{\partial \rho}{\partial t} + \bar{\nabla} \cdot (\bar{u} \rho) = \sum_s m_s \dot{\omega}_s \equiv 0 \quad (20)$$

which is simply an expression of the conservation of mass in the system (i.e. no mass can be created). A similar conservation principle applies to electric charges, i.e. $\sum_s Z_s \dot{\omega}_s \equiv 0$.

The solution procedure of (19) is divided into two parts: (1) the left-hand-side (LHS) of (19) is part of the system of conservation equations of the flow, i.e. the Euler equations generalized to multiple species; (2) the right-hand-side (RHS) makes up the system of chemical kinetics equations. Thus, the rate of change for species s is:

$$\frac{\partial \rho_s}{\partial t} = \left[\frac{\partial \rho_s}{\partial t} \right]_{\text{advection}} + \left[\frac{\partial \rho_s}{\partial t} \right]_{\text{kinetics}} = \left[-\bar{\nabla} \cdot (\bar{u} \rho_s) \right] + m_s \dot{\omega}_s \quad (21)$$

The term due to advection is part of the solution procedure for the Euler equations and does not need to be discussed further here. The term due to chemical kinetics can be described as follows:

$$\dot{\omega}_s = \frac{dN_s}{dt} = \sum_r k_r (v_{(r)s}^R - v_{(r)s}^L) \left(\prod_{s'} (N_{s'})^{\nu_{(r)s'}} \right) \quad (22)$$

where the summation extends over all reaction pathways (r), and the product inside each reaction term extends over all species (s') involved in the chemical reaction. The reaction rate is given by k_r and the coefficients $v_{(r)s'}^R$, $v_{(r)s'}^L$ are the stoichiometric coefficients ("right" and "left") of the reaction. This complex expression can be clarified by considering an example. Consider the following reaction:



The non-trivial stoichiometric coefficients on the left side are:

$$v_{H_2}^L = 1; \quad v_{O_2}^L = 1 \quad (24)$$

Similarly, on the right-side:

$$v_{OH}^R = 2 \quad (25)$$

For this specific reaction, the corresponding rates of change can be written as:

$$\frac{d[H_2]}{dt} = -k_r [H_2][O_2] \quad (26a)$$

$$\frac{d[O_2]}{dt} = -k_r [H_2][O_2] \quad (26b)$$

$$\frac{d[OH]}{dt} = +2k_r [H_2][O_2] \quad (26c)$$

Here the number density variable N_s is replaced by the name of the species in brackets, a common notation used in chemistry, i.e.: $[H_2] \equiv N_{H_2}$.

Consider now the reverse reaction: $OH + OH \rightarrow H_2 + O_2$. The left and right stoichiometric coefficients are now exchanged, yielding the following expressions for the rates of changes of the species densities, *for this reaction only*:

$$\frac{d[H_2]}{dt} = +k_r [OH]^2 \quad (27a)$$

$$\frac{d[O_2]}{dt} = +k_r [OH]^2 \quad (27b)$$

$$\frac{d[OH]}{dt} = -2k_r [OH]^2 \quad (27c)$$

Summing over all reactions, one obtain a system of expressions of the form (for example):

$$\frac{d[N_z]}{dt} = k_1 2[N_a][N_b] + k_2[N_b]^2 - \dots \quad (28)$$

The above can be expressed as:

$$\frac{d}{dt} \begin{bmatrix} N_1 \\ \vdots \\ N_n \end{bmatrix} = \begin{bmatrix} \sum k_r \nu & \dots & \sum k_r \nu \\ \vdots & \ddots & \vdots \\ \sum k_r \nu & \dots & \sum k_r \nu \end{bmatrix} \begin{bmatrix} N_1 \\ \vdots \\ N_n \end{bmatrix} + \begin{bmatrix} \sum k_r \nu & \dots & \sum k_r \nu \\ \vdots & \ddots & \vdots \\ \sum k_r \nu & \dots & \sum k_r \nu \end{bmatrix} \begin{bmatrix} N_1 \\ \vdots \\ N_n \end{bmatrix}^2 + \dots \quad (29)$$

This system can be solved by an implicit method after linearization. The reaction rate k_r is obtained from the Arrhenius equation:

$$k_r = C T^\beta e^{-\theta/T} \quad (30)$$

where k_r is the reaction rate, T is the absolute temperature of the species, C is a constant (frequency factor), β is the fit parameter, and θ is the activation energy (in °Kelvin). The parameter β reflects the dependence of the rate on the average thermal velocity of the molecules and any variation of the reactive cross-section of the collision with respect to energy.

Computational Methodology

The CFD Model

The combustion in a PDE is unsteady in nature. One-dimensional and two-dimensional unsteady CFD computations are used to get realistic approximation of the unsteady processes associated with a PDE operation.

The CFD code *Cafe-Vienna*, developed by Dr. J.-L. Cambier was used to perform the unsteady computations. *Cafe-Vienna* is a Java version of the *Mozart* CFD code (also developed by Dr. Cambier) that computes the inviscid flow field using the Euler equations. An inviscid, two-dimensional numerical scheme coupled to the detailed reaction kinetics of the combustion process is employed. The PDE environment is characterized by multiple shocks in the flow field. Due to extreme sensitivity of the reaction rates to temperature there may be non-physical results or loss of time accuracy even in case of small oscillations. The non-physical oscillations near discontinuities must strictly be avoided, and this requires an upwind scheme. The scheme used here is that of Harten (1983), generalized to multiple species; it is second-order accurate in space, total variation diminishing (TVD), and time accurate¹ (1st-order). The chemical kinetics and the inviscid transport process are coupled via an operator-splitting method.

The fluid flow is coupled with a detailed system of reaction kinetics. In this problem the shortest time scale is usually imposed by the chemistry. Therefore, a fast explicit, numerical scheme for the fluid dynamics, coupled to chemistry by an operator-splitting method is suitable here.

The numerical scheme uses a 7-species (H, O, H₂, O₂, OH, H₂O, and N₂), 18-reaction hydrogen chemistry model. Here, these seven species, the momentum density, and the stagnation energy density are being convected.

¹ First-order time accuracy is sufficient in this case, since usually the time step is small, limited by the chemical time scale.

Boundary Conditions

The walls are considered adiabatic and non-catalytic, with slip boundary conditions. The flow field is occupied by several grids. To ensure continuity, the downstream boundary conditions at each grid are taken as upstream boundary condition for the next grid. The code provides multi-gridding capability. Grids are patched along their common boundaries. The patching process is flux conservative. The boundaries of the external region of the PDE are considered as frozen during the operation.

Numerical Procedure

The first step of a numerical simulation is to discretize the governing equations to reduce the governing partial differential equations to a set of algebraic equations. Conservative property is the key word of this process. Finite volume methods have the conservative property. A finite volume algorithm is employed in the numerical scheme. The finite volume discretization process uses the integral form of the equations, which ensures conservation and correct treatment of the discontinuities [Tannehill (1997)]. Another advantage of this method is that, in the finite volume method, the values of the conserved variables are located within the volume element, not at nodes or surfaces. So the boundary conditions can be applied non-invasively. This method can accommodate complicated surfaces as boundaries. Furthermore the finite volume method can be applied for both a structured and unstructured mesh.

The Euler conservation equations are valid for any arbitrary control volume. By applying Gauss' Theorem over the vector form of Euler equations, the integral form of the conservation equations can be obtained.

$$V \frac{\partial Q}{\partial t} + \int_S \mathbf{F} \cdot d\mathbf{S} = 0 \quad (31)$$

where S is the surface area of the control volume V and $d\mathbf{S}$ is the outward normal from the surface. A finite-volume TVD method is applied in the numerical scheme. The method applied here is very similar to the finite volume TVD method for ideal gases described by Want and Widhopf (1987), except that in the current case an artificial compression term is used. Detailed discussion on this can be found in J.-L Cambier et al. (1988-1989).

An operator-splitting method (loosely coupled method / fractional step method) is used to couple the chemistry to the fluid dynamics. The time accurate operator-splitting method is ideal for unsteady flows. In this method, the non-linear terms of chemical kinetics are dealt with high accuracy. Moreover, individual optimization of the algorithm of each operator is possible due to the flexibility provided by the modular structure of the operator-splitting method. The alternate approach of global splitting method is not used, as it is not time accurate and it is suitable only for the cases where there is less amount of heat release and weak influence of chemical reaction on fluid flow. Moreover to maintain stability and positivity, a large amount of numerical damping is necessary which may cause erroneous results. An explicit operator-splitting method is used in coupling chemistry with fluid dynamics.

The overall scheme is 2nd order accurate in space and 1st order accurate in time. Chemical kinetics is 2nd order accurate in time but due to coupling the overall time-accuracy reduces to the order 1.

CHAPTER 4

CODE VALIDATION & GRID SENSITIVITY ANALYSIS

Code Validation

To establish the accuracy of the current computational method, results for selected cases obtained by the present technique were verified with other published results. Once the accuracy of the method was established, computations were extended for the cases of the current research.

The code validation was performed by comparing the computed results with the experimental results of Schauer et al. (2001). Schauer et al. conducted experiments in a straight PDE tube, which is 914.4 mm long, and 50.8 cm in diameter. In their experiment the authors uniformly filled the PDE tube with a hydrogen-air mixture at various stoichiometric ratios. The simple configuration of Schauer et al. is very easy to model; a one-dimensional model is sufficient to compute the flow inside the PDE tube. The performance of this configuration was computed using one-dimensional CFD with chemical kinetics in the tube and two-dimensional CFD in the external region. A second validation was performed by comparing the same results with the analytical solutions presented by Wintenber et al. (2001), where the authors developed a simple analytical model to approximate the PDE performance.

Figures 3 and 4 show the comparison of the computed values of the specific impulse as a function of equivalence ratio, with the experimental data of Schauer et al. (2001) and with the analytical results of Wintenberger et al. (2001) respectively. The agreement between the experimental performance and computed performance is in general excellent. The computed results are fairly close to the experimental data. In general, the numerical results fall within 9% of the experimentally determined values, except for the cases with very low equivalence ratios. At low values of equivalence ratio, the experimental data show a deviation from a monotonic behavior. This can be explained as a partial failure to complete the combustion at a low stoichiometric ratio. This effect is not reproduced by the computation. The reason is that the spatial resolution is not sufficient enough and the multi-dimensional effects are not modeled. From Figure 4 it can be seen that the computed results and the analytical results of Wintenber et al. (2001) agreed fairly well. In general, the numerical results fall within 9.5% of the analytical results. This simulation validates the current numerical scheme. The overall good agreement with the experimental and analytical results gave confidence about the accuracy of the current numerical method.

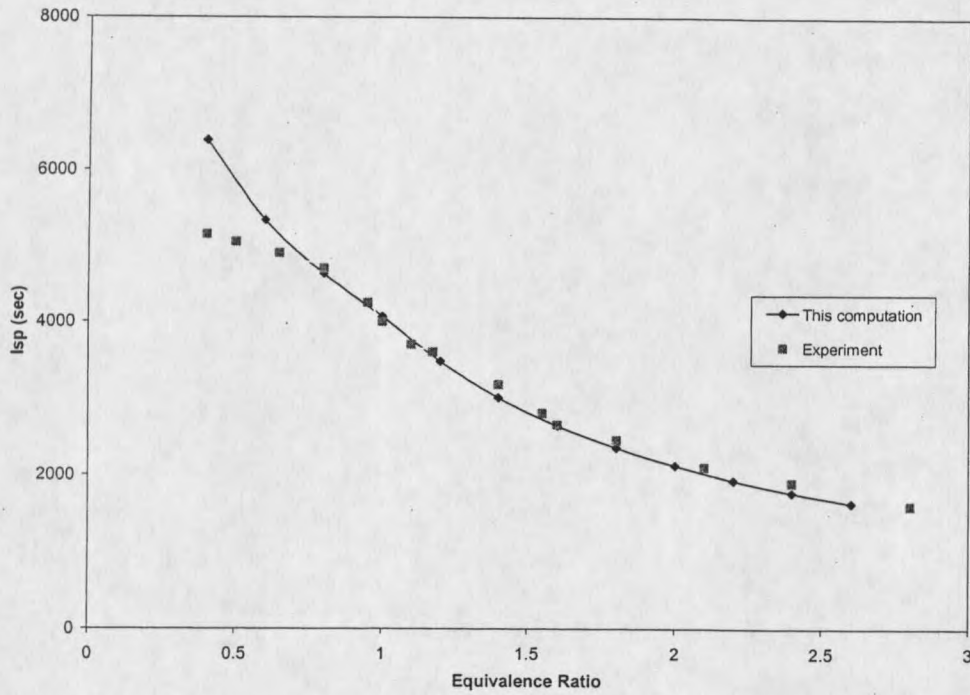


Figure 3. Specific impulse compared to the experimental results of Schauer et al. (2001)

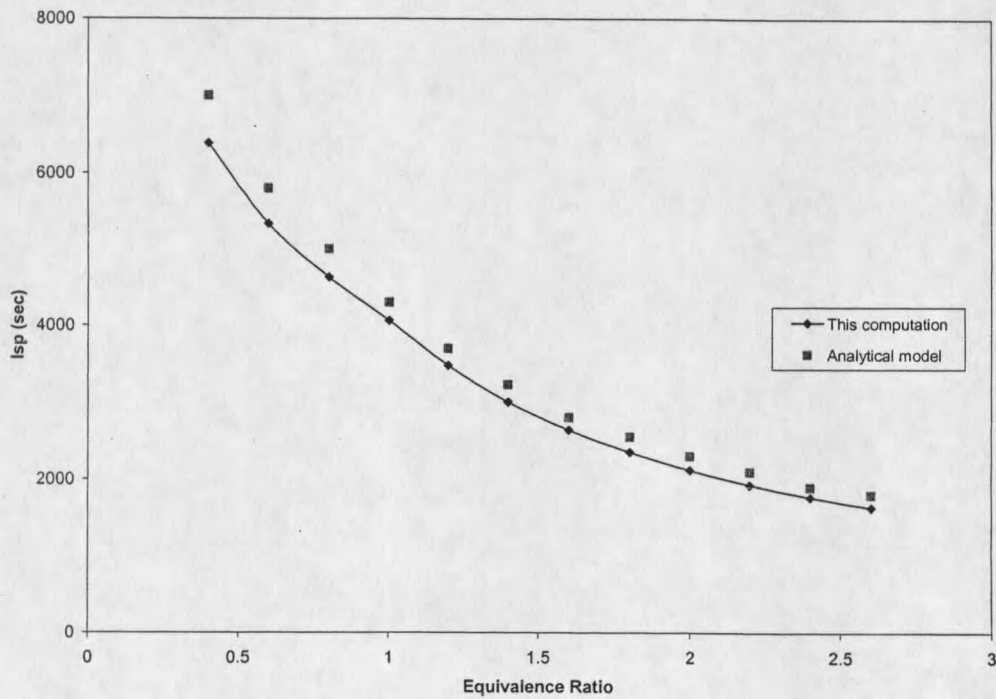


Figure 4. Specific impulse compared to the analytical predictions of Wintenberger et al. (2001)

Grid Sensitivity Studies

In order to minimize the computation time with a desired level of accuracy, the grid independence test is essential. The computational time increases with an increase in the number of grids. On the other hand, a coarser grid may give misleading results. The grid resolution should ensure that the main detonation features such as detonation speed, temperature, and pressure distributions behind the detonation shock etc. are grid independent, as well as ensure that the computational cost is minimum. Four different cases with different grid resolutions were run to establish the grid independence.

In this test, the system configuration is a straight cylindrical tube with constant cross-section, 20 cm in length and 4 cm in diameter. Using four different uniform grid sizes, one-dimensional simulations were carried out. The different grid sizes are: 1, 0.8, 0.4, and 0.2 mm. The initial conditions were kept the same for all the cases.

Table 1. Different Grid Resolutions

Grid	Grid Size (mm)	Number of elements
A	1	200
B	0.8	250
C	0.4	500
D	0.2	1000

Figure 5 shows the detonation wave profiles resulting from four different grid sizes. From this figure it is clear that for the different grid spacings all the simulations show very similar detonation behavior. In general, the results with the coarsest grid (grid size 1 mm) fall within 7% of the results obtained using the finest grid (grid size 0.2 mm), except in the region near the peak pressure. Figure 6 shows the PDE chamber pressure history for different grid resolutions. From the results it is evident that the computed performances are reasonably independent of the grid resolution. Therefore, it can be concluded that reliable solutions can be obtained with different grid resolutions. If both accuracy and computational time are taken into account then the grid size of 1 mm can be a reasonable choice. Therefore, the grid with 1 mm element size was chosen for the current study.

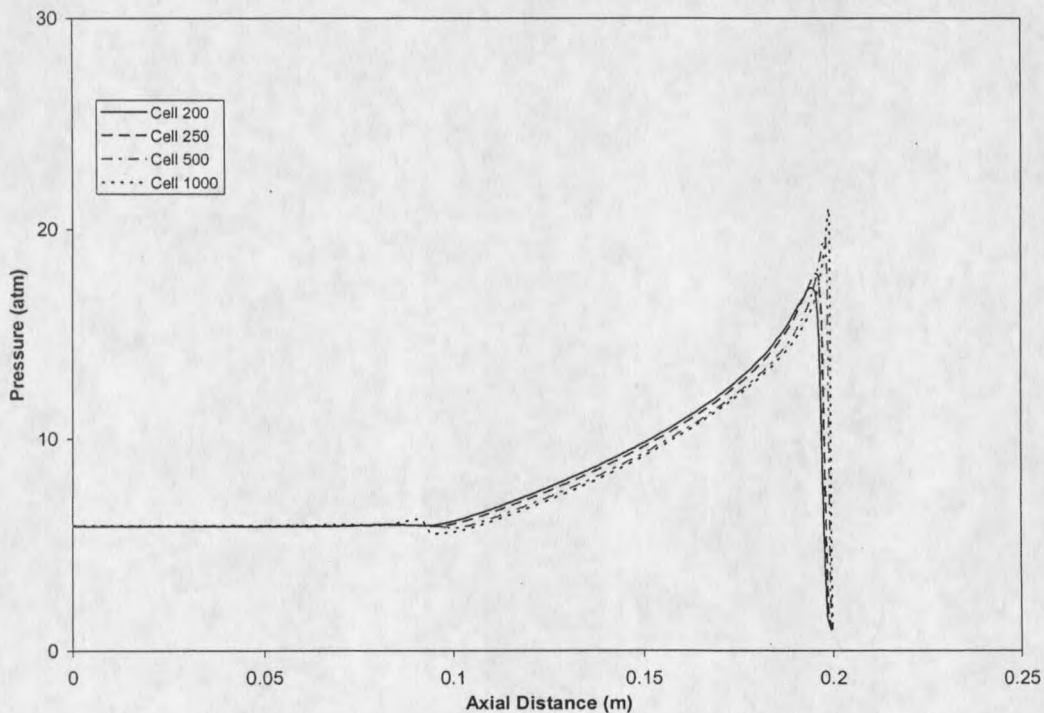


Figure 5. Pressure profiles for different grid resolutions

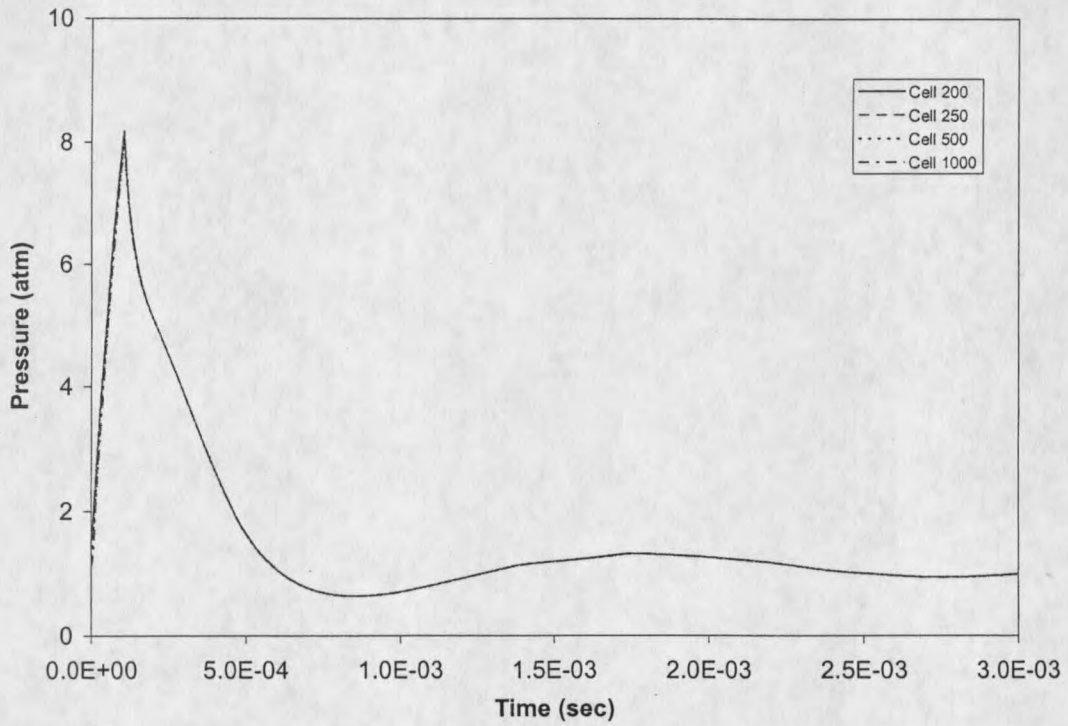


Figure 6. PDE pressure history for different grid resolutions

CHAPTER 5

RESULTS AND DISCUSSION

The numerical results presented in this chapter were obtained using a modified version of a Java-based performance optimization software named *Cafe-Vienna*. The CFD code *Cafe-Vienna* was employed to perform the unsteady computations. Accuracy of this code was tested by comparing the results with experimental results of Schauer et al. (2001) and with the analytical solutions reported by Wintenberger et al. (2001). Furthermore, grid independency tests were carried out to ensure that the chosen grid provides accurate results within an acceptable computational time.

The primary objective of this research was to elucidate the propulsive performance characteristics of the PDE over a wide range of operating conditions. The results of a systematic numerical investigation of PDE performance characteristics have been presented in the following sections. Hydrogen is taken as the fuel in the current study, since the chemistry of hydrogen-air combustion is fairly well established. This also allows comparing the results of the current study with the other published results.

Following Zitoun and Desbordes (1999), four characteristics are used to analyze the propulsive performance of the PDE: thrust, impulse, impulse per unit volume, and specific impulse. The pressure differential, caused by the detonation wave, creates an unsteady thrust. Thrust is generated as long as the pressure inside the

PDE tube is greater than the ambient pressure. It can be computed by integrating the pressure-differential on the thrust-wall over the entire surface of the thrust-wall.

$$F(t) = \int_A \Delta p(t) dA \quad (32)$$

Where, $F(t)$ is the generated thrust, $\Delta p(t)$ is the pressure differential over the thrust-wall and A is the area of the thrust-wall. One of the most important performance parameters of the PDE is the impulse generated per unit cycle, which can be computed by integrating the thrust over the cycle time:

$$I(t) = \int F(t) dt \quad (33)$$

The resulting impulse can be expressed in two ways: impulse per unit volume and impulse per unit mass. The impulse per unit volume (I_v) is defined as the ratio of the single-cycle impulse to the volume of the tube. Impulse per unit volume is independent of the tube size.

$$I_v = \frac{I}{V_{pde}} \quad (34)$$

Specific impulse (I_{sp}) is used as a performance parameter of an air-breathing pulsed detonation engine. It is defined as the ratio of the single cycle impulse to the product of the fuel mass and the earth's gravitational acceleration g :

$$I_{sp} = \frac{I}{M_{fuel} g} \quad (35)$$

The specific impulse is used as a figure of merit in the propulsion community. Like impulse per unit volume, the specific impulse is size-independent. It can be used less ambiguously than impulse since it does not directly depend on the PDE tube size.

Computations can be performed using two approaches: (1) with a full coupling to chemical kinetics of combustion and (2) with a global chemical equilibrium model. In the first approach, the detonation is initiated (computationally) at the closed-end of the PDE tube and it travels through the PDE tube, initiating chemical reactions. The flow field is coupled at all times with the detailed systems of reaction kinetics. In the case of the chemical equilibrium model, there is no need of detonation initiation; chemical equilibrium is assumed in the *entire* tube at the time of ignition. This is equivalent to instantaneous constant-volume combustion of the mixture. The burned gases are then subjected to a blow-down process during which no reaction occurs between the species.

In the next section, the effects of the PDE tube length will be discussed. It will be followed by the effects of initial conditions, nozzle effects, and mixture effects.

Effects of Tube Length

This section examines the effects of tube length on the performance of a pulse detonation engine. Here, the system consists of a straight cylindrical tube with constant cross-section. The tube, open at one end and closed at the other, is uniformly filled with a stagnant propellant mixture. A stoichiometric hydrogen-air mixture is used as the propellant. Detonation is initiated by depositing a large amount of energy

near the closed end. This is achieved by creating a high pressure and high temperature region near the closed end, where temperature and pressure are set at 1500 K and 10 atm respectively. Both the ambient pressure and the initial fill pressure are set at 1 atm. Studies were performed for a single pulse in a two dimensional axi-symmetric configuration.

Figure 7 shows the schematic of the computed configuration. As the configuration is simple, it is modeled using an internal one-dimensional grid. The length of the PDE tube is systematically varied, whereas the cross-sectional area is kept constant. Numerical results were obtained for the following sets of input data:

$$L_{pde}=20, 30, 40, 60, 80 \text{ cm}$$

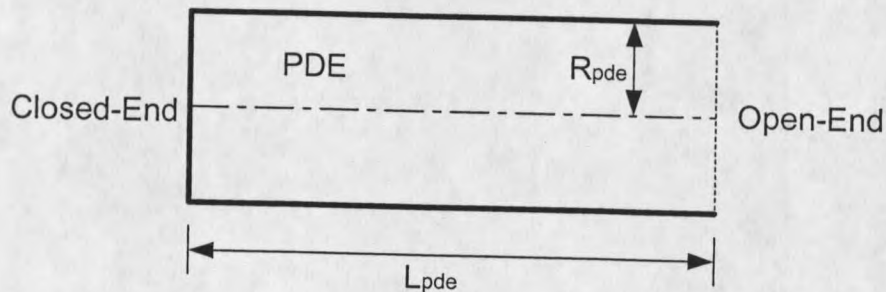


Figure 7. Schematic of a pulse detonation engine

Figures 8 and 9 show the total thrust and the total impulse as functions of time for different PDE tube lengths. It is evident from the results that an increase in PDE tube length prolongs the thrust generation and increases the total impulse. A closer look at the thrust profiles reveals that for the 30 cm long tube, a positive thrust is generated for approximately 0.9 ms; whereas for the higher values of tube length (40 cm and 60 cm), this time is approximately 1.2 ms and 1.8 ms respectively. This

indicates an increase in the thrust generation time when the PDE tube is longer. The prolonged thrust generation in the case of longer PDE tubes is due to the fact that longer tubes contain more fuel, and therefore more thrust is produced. From the impulse profiles (Figure 9) it can be seen that for the 30 cm long tube, the maximum impulse is approximately 0.36 N-s. For the 40 cm long tube, the maximum impulse is approximately 0.48 N-s, which is about 33% higher than the previous case. The higher impulse is caused by the prolonged thrust generation as shown in the thrust profiles.

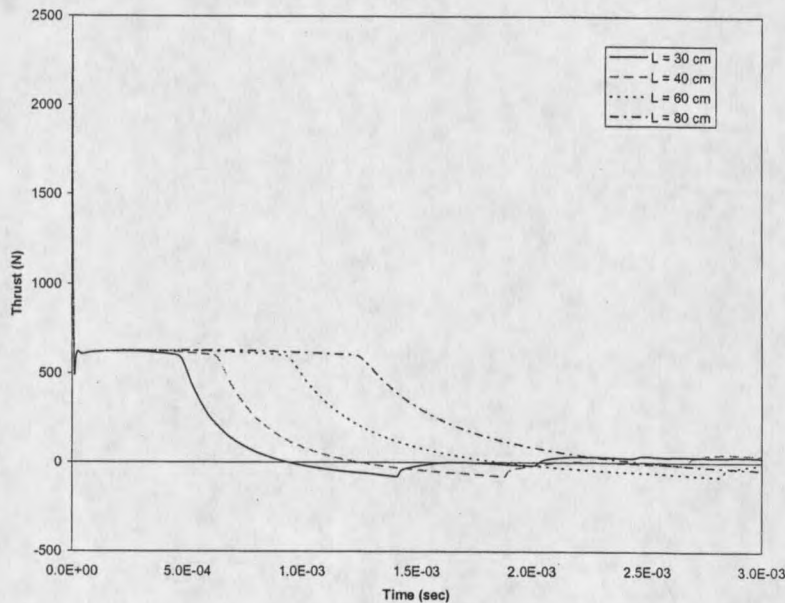


Figure 8. Instantaneous thrust profile for different tube lengths

Figure 10 shows the maximum impulse, generated during a single pulse, as a function of tube length. The results indicate a linear increment of the total impulse with the tube length. This is due to the fact that when the tube length is increased the fuel mass increases proportionately, resulting in a proportional increase in the impulse

generation. The results of the simulations are in good qualitative agreement with the experimental results of Zitoun et al. (1999).

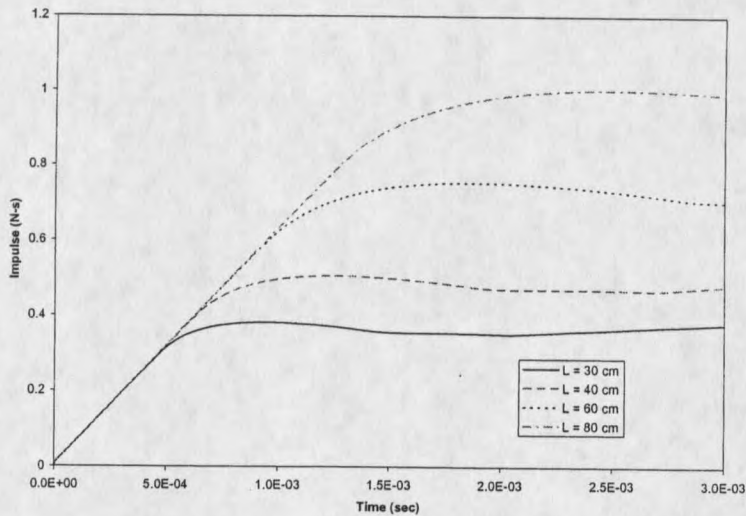


Figure 9. Impulse trace for different tube lengths

As already noted, the specific impulse is independent of the amount of fuel used and the volume of PDE tube. Therefore, although the impulse level increases nearly linearly with tube length, the impulse per unit mass of fuel (or, the specific impulse) should remain the same. Figure 11 shows the specific impulse as a function of tube length. The results indicate that the specific impulse is almost independent of the tube length, as expected. The small increase of I_{sp} with the tube length is due to the fact that if the tube length is increased, the gas resides in the tube for longer times (it takes longer for the rarefaction waves to travel back and forth down the tube) until the pressure has dropped to ambient values. As the gas is perturbed by the rarefaction, it cools (adiabatically) from the post-detonation conditions. The lower temperature would shift the chemistry towards slightly lower dissociation level (i.e. the gas will

recombine a little more). However, this process takes some time and if the tube is short there is less time to achieve this new equilibrium state. In a longer tube, this process can be completed and there is a slight increase in chemical energy release during the blow-down.

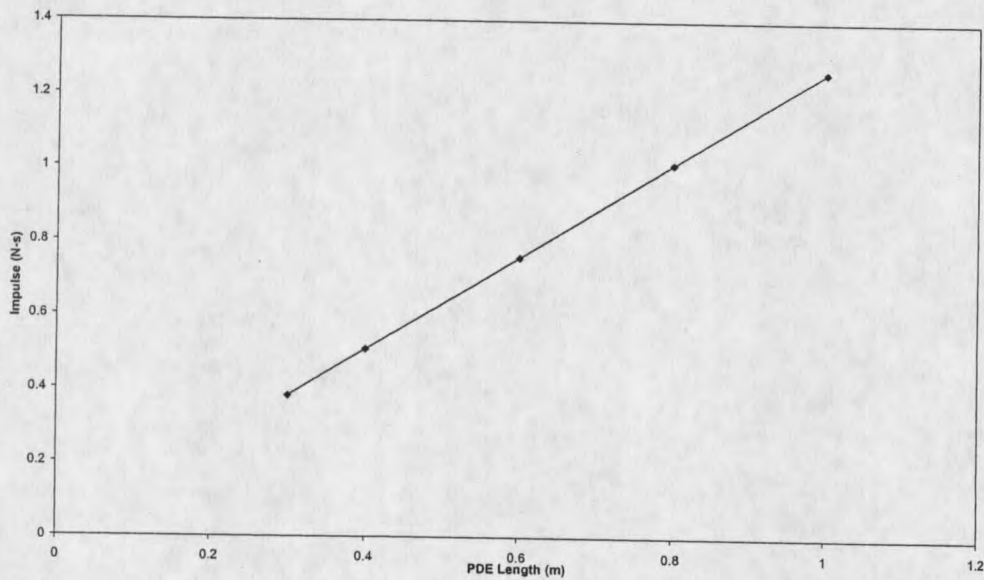


Figure 10. Variation of maximum impulse of a cycle with PDE tube length

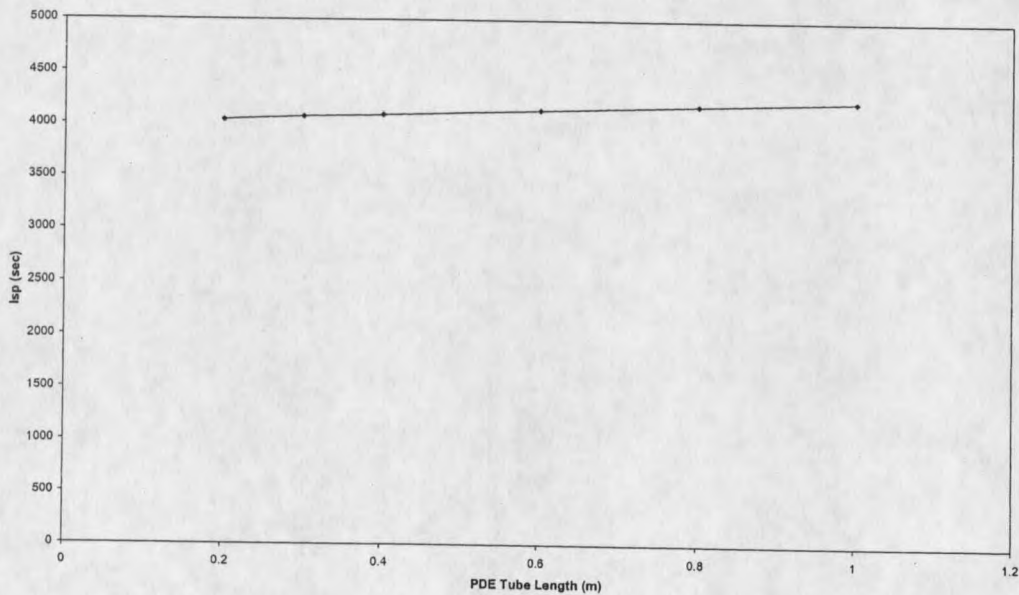


Figure 11. Variation of specific impulse with respect to PDE tube length

Effects of the Fill Pressure

The fill pressure inside a PDE tube is one of the initial parameters whose effects need to be investigated. The fill pressure may considerably affect the performance of a pulse detonation engine. The effects of initial fill pressure on PDE performance was first examined by Wintenberger et al. (2001), who used a simple analytical model to predict the PDE performance. In this section, the results of the numerical method are compared with the analytical solutions presented by Wintenberger et al. (2001). This will provide a validation for the numerical scheme and will also help in understanding the results.

To study the effects of the initial chamber pressure a number of simulations were performed over a range of fill pressures. The numerical results were obtained for the following sets of input data, where the initial chamber fill pressure was increased in steps and all other parameters were kept constant:

$$P = 0.2, 0.4, 0.6, 0.8, 1.0, 1.2, 1.4, 1.6, 1.8, 2 \text{ atm.}$$

Impulse per unit volume and specific impulse were computed for all of the cases. Figure 12 shows the impulse per unit volume (I_v) as a function of the fill pressure. From the results it is evident that the impulse per unit volume scales linearly with the fill pressure. This is due to the fact that the generated impulse should scale linearly with the mass of the propellant mixture which is directly proportional to the fill pressure. According to the Equation of State of the system, as described in Chapter 3, an increase in the fill pressure results in an increase in fuel density, and

hence results in an increased mass of fuel inside the PDE combustor. Therefore, the total impulse generation increases.

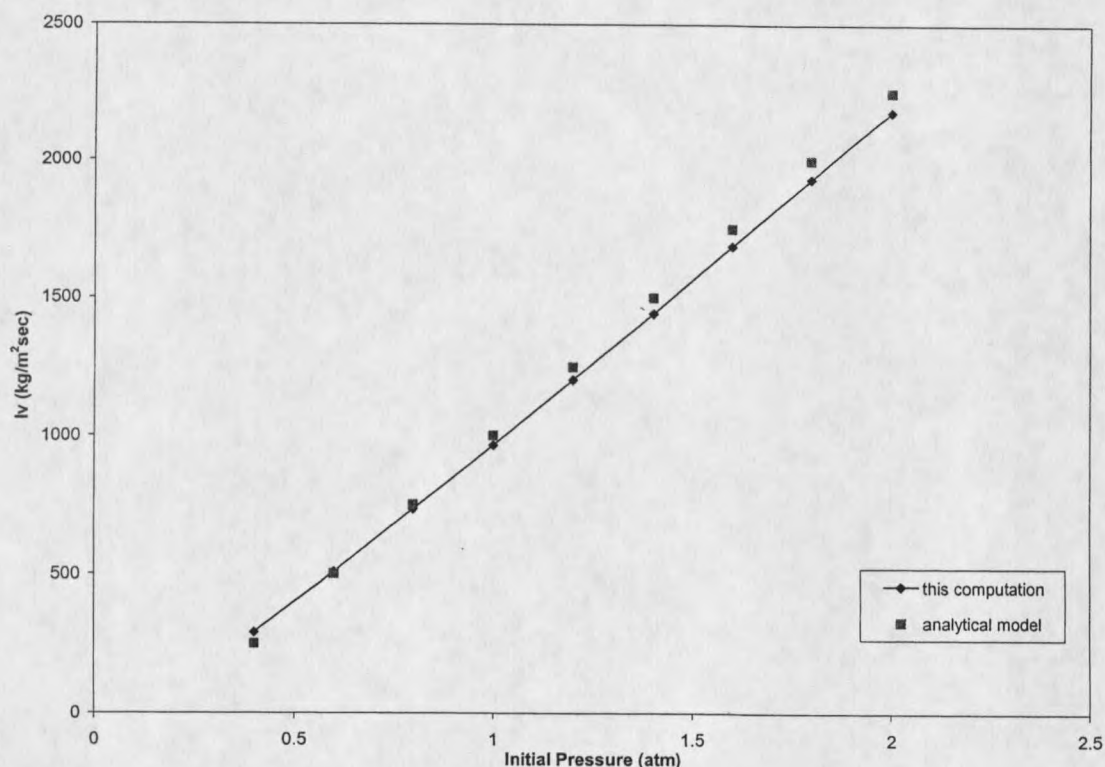


Figure 12. Impulse per unit volume comparison between numerical results and analytical results of Wintenberger et al. (2001), for varying fill pressure

Figure 13 illustrates the variation of the specific impulse (I_{sp}) with the fill pressure. The results indicate that the fill pressure plays a positive role for the specific impulse. Following Cambier et al. (2003), in an ideal situation, the specific impulse should be independent of fuel density and fill pressure. From the I_{sp} curve a steady growth of the specific impulse was observed. This steady increase of the I_{sp} indicates a scaling deviation which is due to a higher degree of recombination of the reacting

gases at a high pressure. In other words, at low density there are a lot of dissociated products, and at high density these dissociated products recombine. As the density or pressure increases, the higher amount of recombination implies that there is more chemical energy extracted from the fuel, and the performance (I_{sp}) increases.

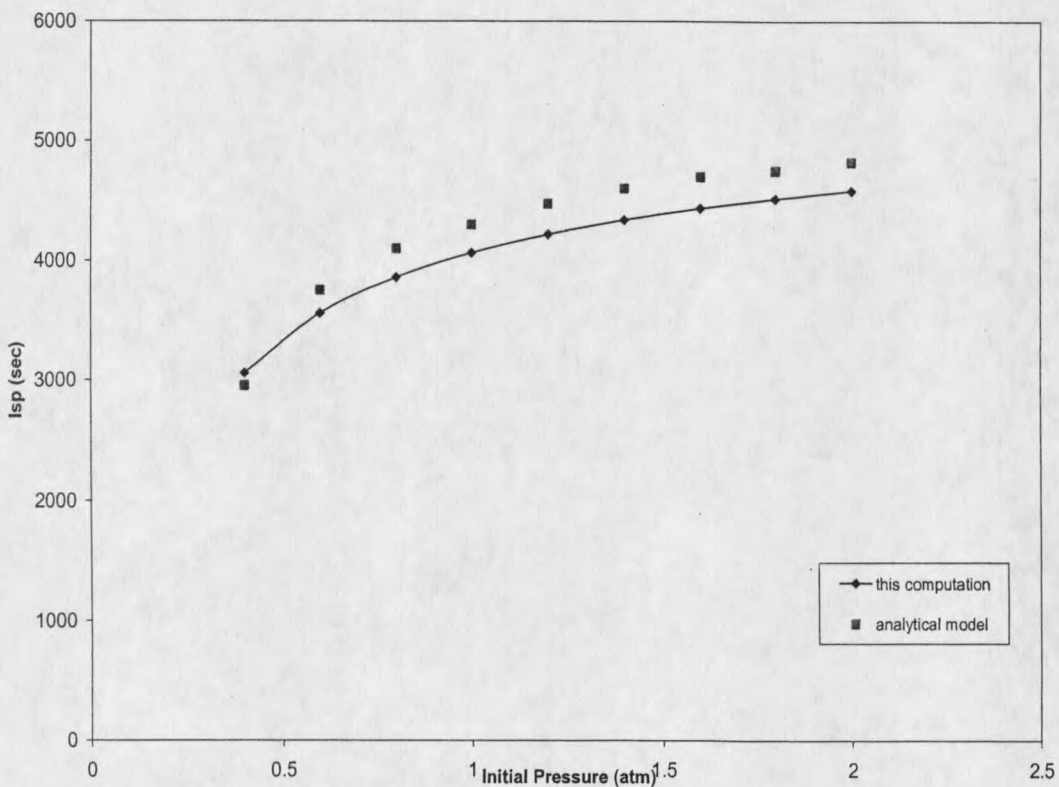


Figure 13. Specific impulse comparison between numerical results and analytical results of Wintenberger et al. (2001), for varying fill pressure

As shown in Figure 12 and Figure 13, the results of the simulation and Wintenberger et al.'s (2001) analytical results agree fairly well. In general, the numerical results fall within 7% of the predicted analytical values.

Effects of the Initial Temperature

The initial temperature of the propellant mixture can affect the impulse of a PDE. Therefore, it is necessary to examine the PDE performance when the combustor is filled with high temperature propellants instead of a cold and dense propellant mixture. In this investigation, a number of simulations were performed and the results were analyzed in terms of temperature effects on various PDE performance characteristics. The numerical results were obtained for the following sets of input data, as shown in Table 2, where the initial chamber temperature was increased in steps for different initial fill pressures. All other parameters were kept constant.

Table 2. Input data

Fill Pressure	Initial Temperature
1 atm	300 K
	400 K
	500 K
	600 K
2 atm	300 K
	400 K
	500 K
	600 K
3 atm	300 K
	400 K
	500 K
	600 K

For all of the cases, impulse per unit volume and specific impulse were computed. The results obtained indicate that the impulse per unit volume is greatly affected by the initial temperature, whereas the specific impulse is not significantly

affected by the initial temperature of the propellant mixture. Figure 14 shows the impulse per unit volume (I_v) as a function of the initial temperature for different chamber fill pressures. The results show that I_v gradually decreases as the initial temperature increases. This is because the impulse per unit volume scales linearly with the initial density of the propellant mixture which is inversely proportional to the temperature (when the initial chamber pressure is kept constant). According to the Equation of State of the system, as described in Chapter 3, an increase in the initial temperature results in a decrease in fuel density, and hence results in a decrease in fuel mass inside the combustor. As a result, the total impulse generation decreases, as shown in the I_v curve.

Figure 15 illustrates the variation of the specific impulse (I_{sp}) with the initial temperature. The results indicate a very slow decrease of the specific performance with the initial temperature. This small scaling deviation is caused by a phenomenon called endothermic dissociation. High temperatures cause a considerable amount of dissociation, which leads to a loss in the heat release from the combustion process. Therefore, a lesser amount of chemical energy is extracted from the fuel at a higher reactant temperature, and this results in a decrease in the specific performance. The results of the simulation are in agreement with this explanation. The I_{sp} curve indicates that when the initial propellant temperature is 300 K and the fill pressure is 1 atm, the I_{sp} is approximately 4200 sec. If a propellant mixture with an initial temperature of 400 K is used, the I_{sp} value drops to approximately 3900 sec, which is about 7.3 % lower than the previous case. As discussed above, this decrease in the

specific impulse is due to dissociation loss. Therefore, the theory and the numerical results are in agreement throughout this investigation.

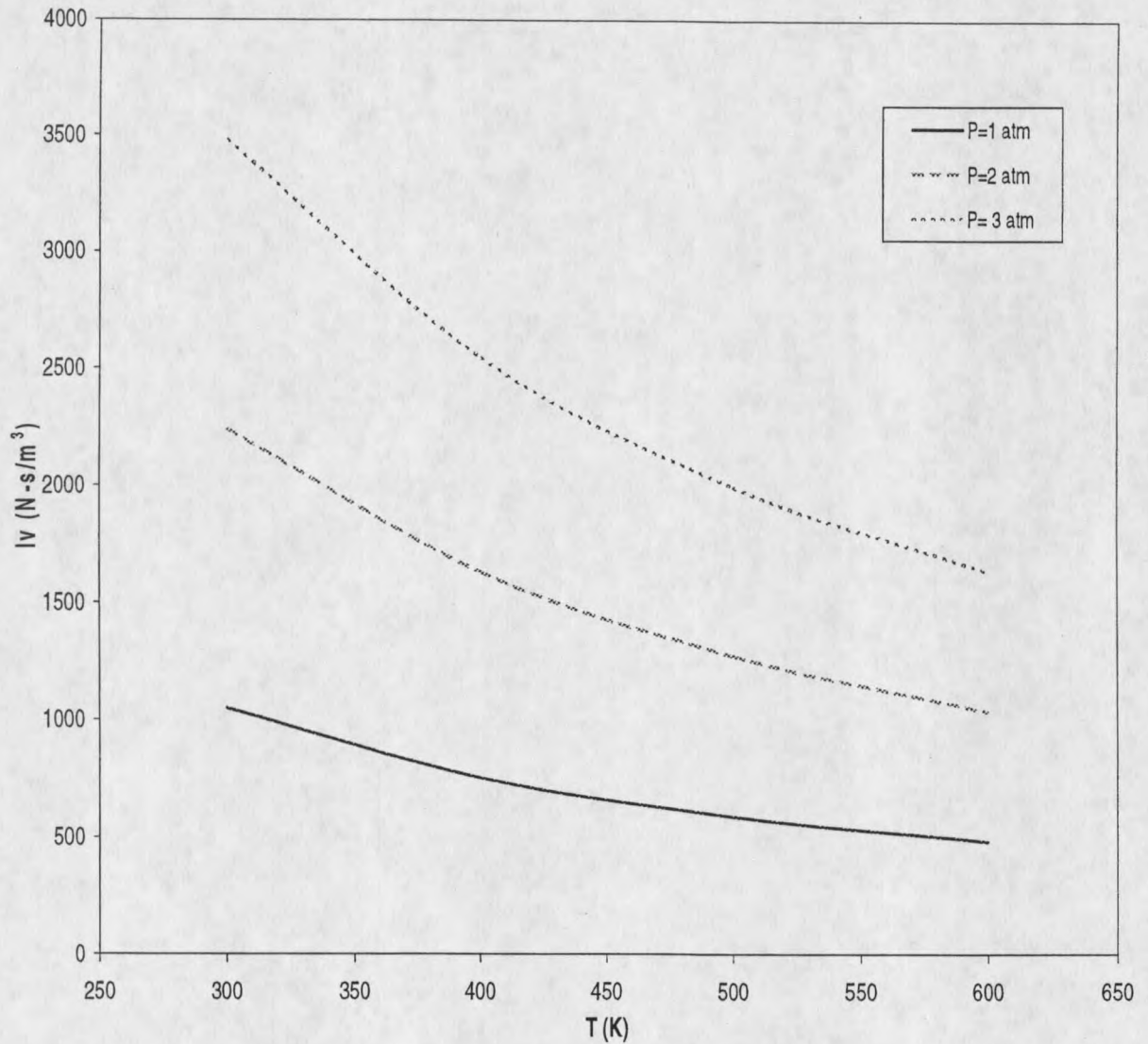


Figure 14. Impulse per unit volume versus initial temperature for different filling pressures

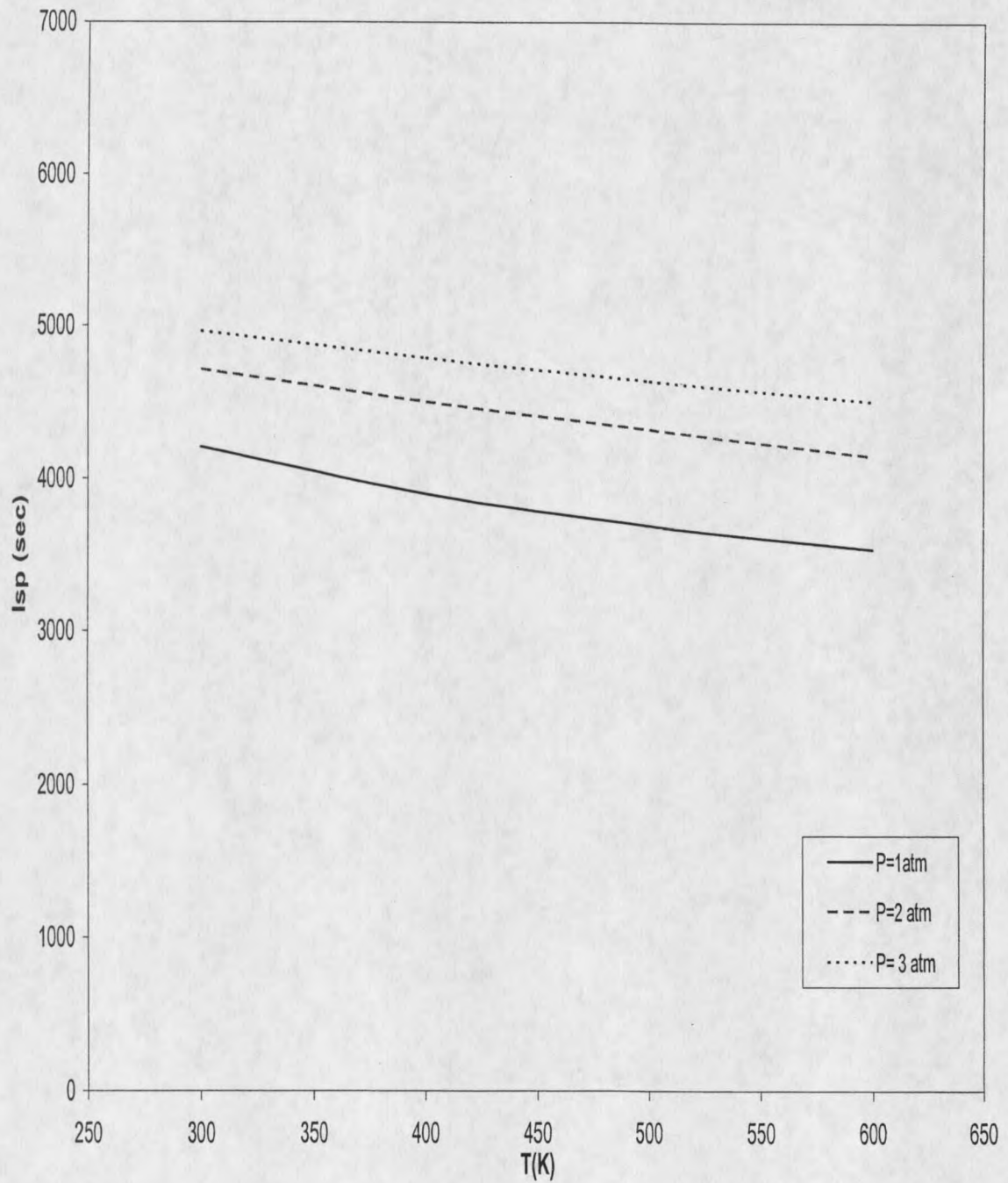


Figure 15. Specific Impulse versus initial temperature for different filling pressures

Effects of Tube Fill Fraction

This section examines the effects of the size of the propellant mixture. Figure 16 shows a schematic of the computed configuration where the PDE tube (of length L_{pde}) is not completely filled with the propellant mixture. The propellant mixture occupies the length $l_{propellant}$ of the PDE tube and the remaining portion is filled with air. The tube fill fraction (TFF) is the ratio of the volume of the propellant mixture to the volume of the PDE tube. When the tube fill fraction ($l_{propellant}/L_{pde}$) is 1.0, the tube is completely filled with a fresh propellant mixture. At a chamber fill fraction of less than 1.0, the tube is partially filled with a fresh reactant mixture and the remaining portion of the tube is filled with air. Here the performance characteristics are presented as functions of the tube fill fraction.

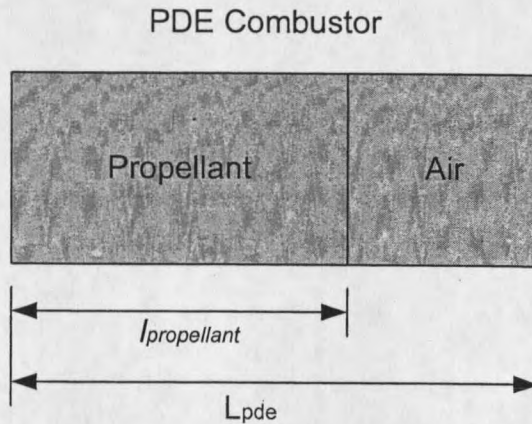


Figure 16. Schematic of the straight tube PDE with partial tube filling

In this investigation detonation was initiated at the closed-end of the tube, by raising the temperature and pressure in the region adjacent to the left wall at 1500 K

and 10 atm respectively. Studies were performed for a single pulse in a two-dimensional axi-symmetric configuration. Initial temperature within the chamber was set at 300 K and both the initial fill pressure and the ambient pressure were set at 1 atm.

To study the effects of the tube fill fraction a number of 1-D simulations were performed over a range of values of $l_{\text{propellant}}$. The numerical results were obtained for the following set of input data, where $l_{\text{propellant}}$ was increased in steps and all other parameters were kept constant:

$$\frac{l_{\text{propellant}}}{L_{\text{pde}}} = 0.25, 0.3, 0.35, 0.4, .45, 0.5, 0.55, 0.6, .65, 0.7, .75, 0.8, 0.85, 0.9, 0.95, 1.0$$

Figure 17 shows the thrust generated during a single pulse as a function of time. The initial spike is due to the deposition of high energy near the closed-end of the tube. From the figure it is evident that in the case of full tube filling the thrust is produced for a longer time than the partial tube fill cases. This is because a higher value of tube fill fraction means more fuel, which generates more thrust. Figure 18 shows the total impulse as a function of time for different tube fill fractions. It can be seen that the amplitude of the impulse profile increases with the increase of tube fill fraction. This higher impulse is due to the prolonged thrust generation at a higher value of tube fraction, as seen in the thrust profiles.

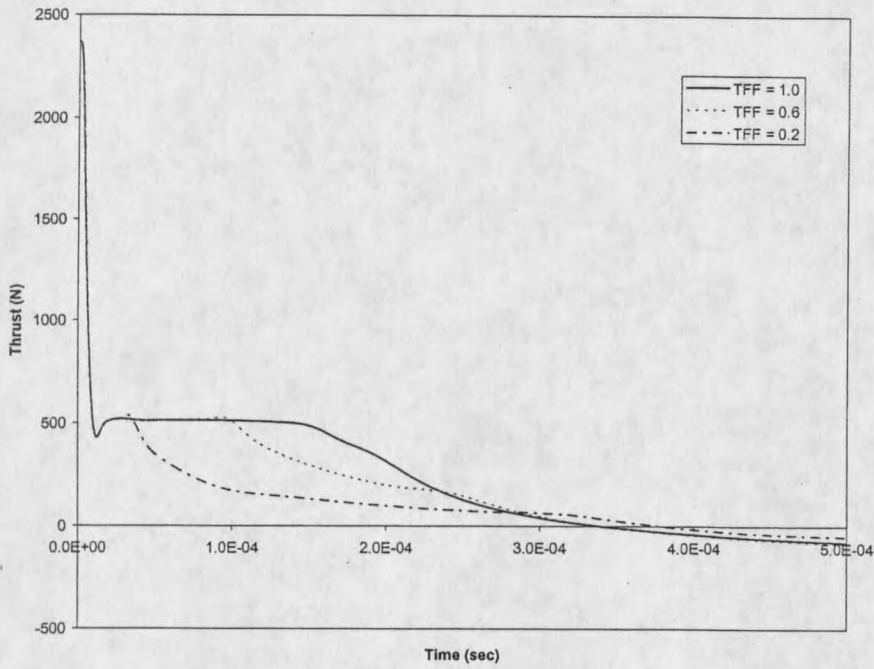


Figure 17. Thrust profiles for different tube fill fractions (TFF)

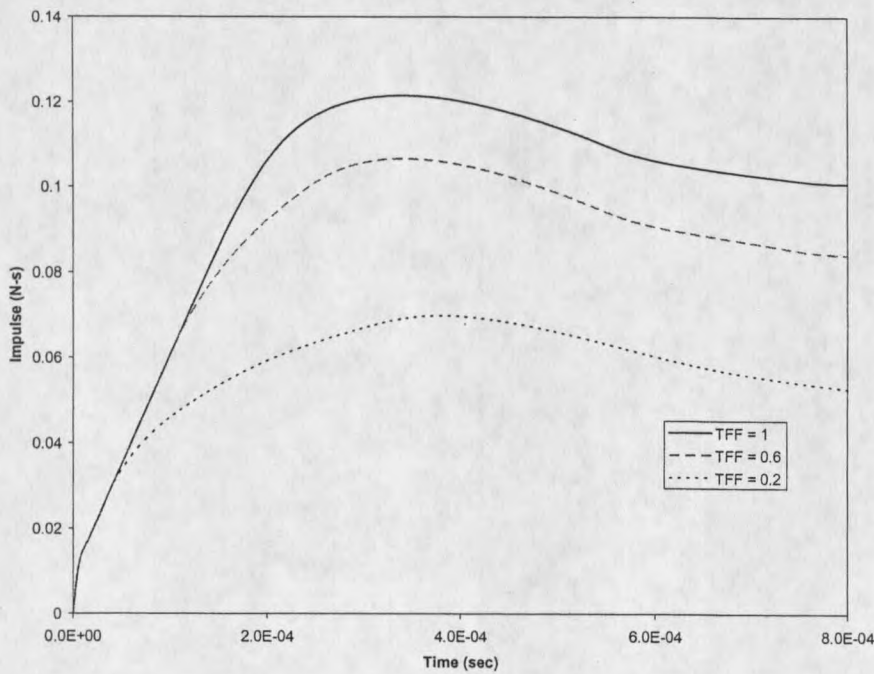


Figure 18. Impulse profiles for different tube fill fractions

Figure 19 shows the final impulse during a single pulse as a function of the chamber fill fraction. The impulse is observed to increase gradually with the chamber fill fraction, and it reaches the maximum value when the tube fill fraction is equal to 1. From Figure 19 it can be seen that when the PDE tube is fully filled with the propellant mixture (i.e. TFF = 1), the impulse is approximately 0.14 N-s. For the cases of 75% and 50% tube fill fractions, the impulse is 0.13 N-s and 0.11 N-s respectively. The results indicate that a 25% reduction of the mixture size leads to a decrease of impulse by only 9.3%; a 50% reduction of mixture size leads to a decrease of impulse by only 27.7%. Therefore, the impulse generation is not proportional to the degree of tube fill. It is interesting to observe that more than 50% of the maximum impulse (generated during the full-filling case) can be obtained by filling only 30% of the tube with the propellant mixture. This results in a lower fuel consumption and better specific impulse.

The variation of the specific impulse (I_{sp}) with the tube fill fraction (TFF) is shown in Figure 20. As shown in this figure, increasing the volume of the reactive gas mixture plays a negative role in the specific impulse. For the values of tube fill fraction 1, 0.75, and 0.50, the I_{sp} values are approximately 5325 sec, 6000 sec, and 7250 sec respectively. The results indicate that a 25 % reduction of the propellant mixture size leads to an I_{sp} increase by approximately 18 %; a 50 % reduction leads to an I_{sp} increase by approximately 36 %. This trend has been confirmed by the experimental observations of Schauer et al. (2001). One possible reason for this increase in the specific impulse is that when a tube is partially filled with propellant

mixture, the remaining portion will act as a straight nozzle for the exhaust of the detonation products. As discussed in the section on nozzle effects, the presence of a straight nozzle with a PDE tube can significantly increase the PDE performance; the performance increases with the length of the straight nozzle. A detailed analysis of the effects of a straight nozzle can be found in the following section.

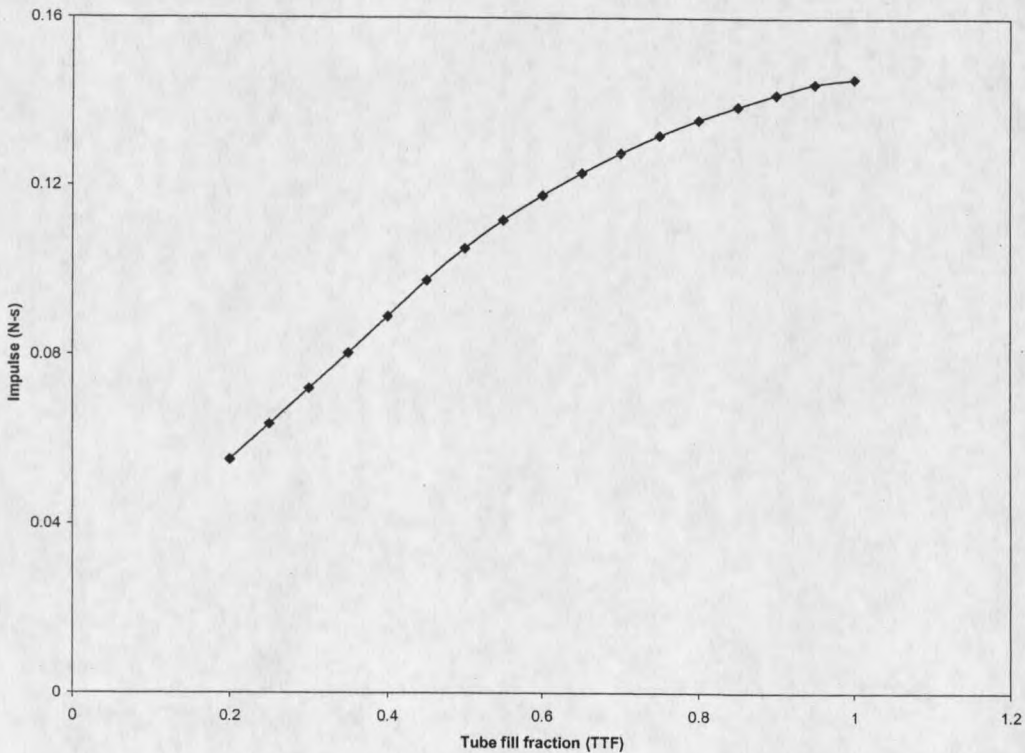


Figure 19. Impulse versus tube fill fraction

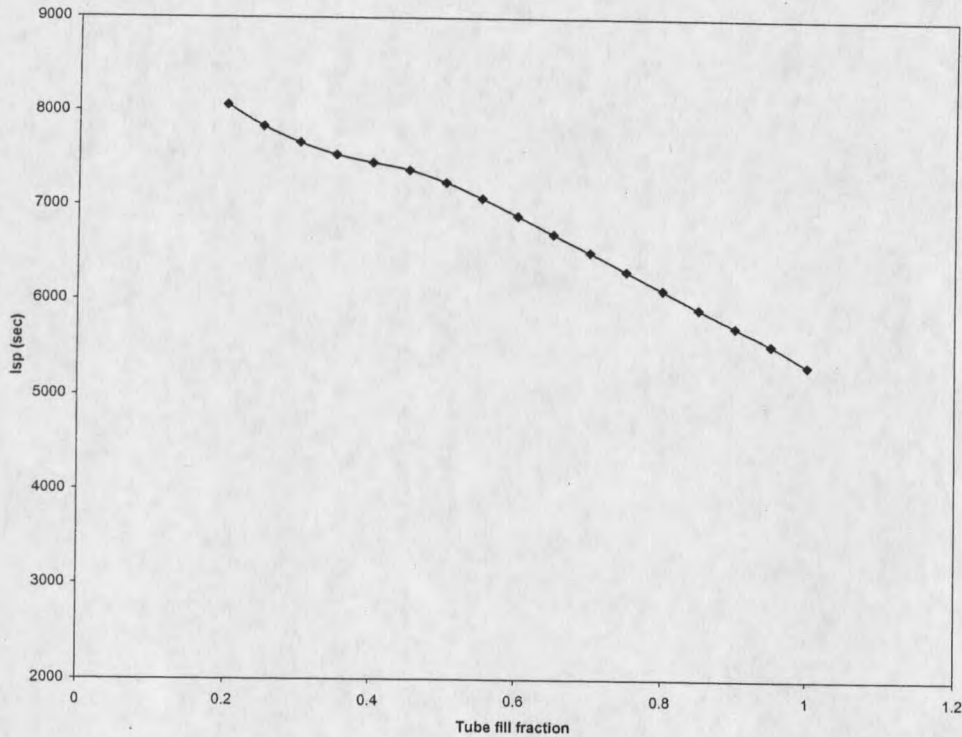


Figure 20. Specific impulse versus tube fill fraction

The gain in specific impulse in the case of partial tube filling is valid if the non-combustible section of the PDE tube is filled with cold and dense air. It is important to observe the effect of the air temperature in the noncombustible section. This effect is particularly important at high flight number, as the inlet air must be decelerated to near stagnation temperature. For the current configuration, a 100 cm long PDE tube is partially filled with stoichiometric hydrogen-air mixture. The filling length of the detonable hydrogen-air mixture is 76 cm; the remaining portion is filled with air. The temperature of the air of the non-combustible section is systematically varied. A series of computations were performed for the air temperature – 350, 600, 900, 1200, 1500, and 1800 K.

Figure 21 shows the specific impulse as a function of air temperature. As shown in the figure, the specific impulse is greatly affected by the air temperature in the non-combustible section. The specific impulse monotonically decreases with the air temperature. If the noncombustible section of the tube were filled with high temperature combustion products, the gain in the specific impulse would be minimal. It is not yet clear how to characterize the exact dependence of the performance on the air quality. It can be reasonably assumed that the acoustic impedance in the air section plays a critical role here.

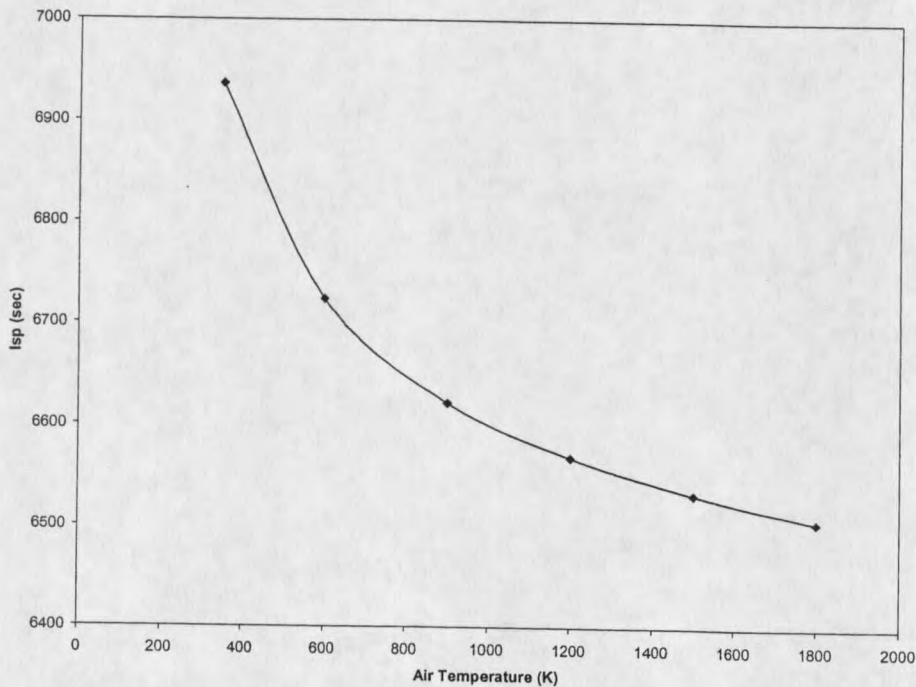


Figure 21. Specific impulse versus temperature of air in stratified charge

Also observed was the pressure profile behind the moving detonation wave while the detonation wave remained inside the PDE tube's non-combustible air section. Figure 22 shows the pressure profile inside a 100 cm long PDE tube, with a

tube fill fraction of 0.6 at the times 0.026 ms and 0.064 ms. It can be observed that at 0.026 ms the detonation wave stays approximately 50 cm away from the thrust wall. Since the filling length is 60 cm, the shock front is still inside the propellant mixture. From the pressure profile it can be seen that the peak pressure behind the shock is 13 atm. When the detonation wave enters the non-reactive air section the detonation is quenched, and the shock loses its strength as it no longer receives energy support from the chemical reactions. Figure 22 shows the pressure profile behind the quenched shock when the shock reaches near the tube-exit at approximately 0.064 ms. It can be seen that the peak pressure behind this quenched shock is only about 8 atm, which is considerably lower than the pressure behind the original shock front.

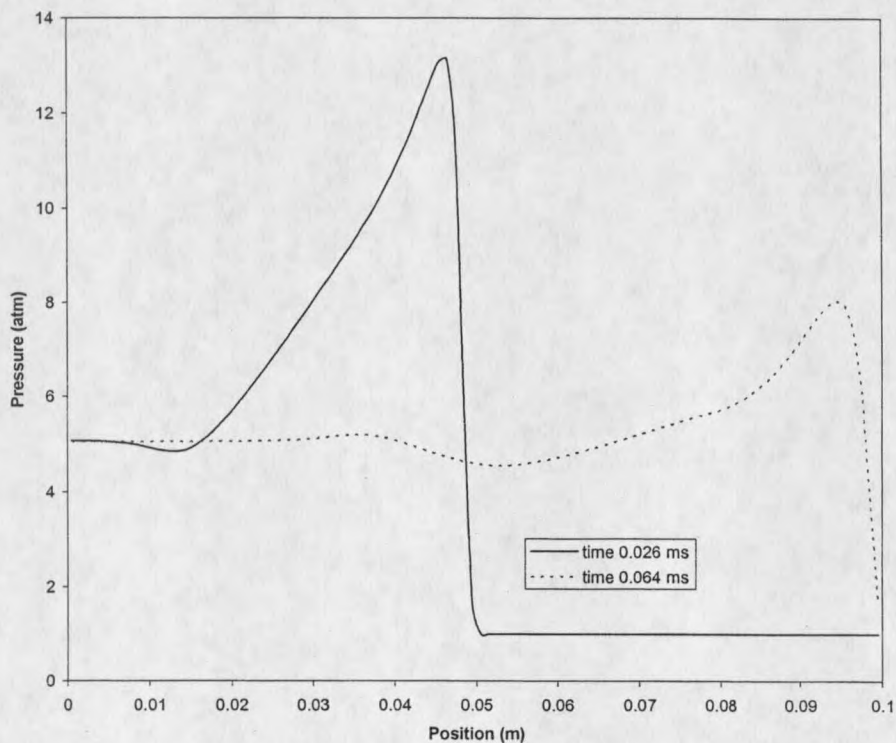


Figure 22. Pressure profile at two different times for tube fill fraction 0.6

Effects of Nozzle Geometry

A nozzle is an indispensable component of conventional steady flow propulsion engines. In the case of rocket engines, converging-diverging nozzles are used for steady conversion of thermal energy to kinetic energy in the supersonic flow downstream of the throat. In the pulse detonation engine (PDE) the conversion of thermal energy to kinetic energy is achieved through waves. The performance of the nozzle of a rocket engine is optimized when the pressure at the nozzle exit plane is the same as the ambient pressure. However, this simple criterion is not applicable for optimizing the performance of the PDE nozzle. The operation of the PDE is unsteady in nature and the pressure field at the nozzle exit plane is also unsteady making the problem of nozzle optimization difficult. Moreover, due to the complexity of the diffraction of a detonation wave through a nozzle, the effects of a nozzle on PDE performance are not yet fully understood. The operation of the PDE is cyclic in nature. The PDE performance can be optimized by reducing the cycle time. The presence of a nozzle may affect the time required to drop the pressure inside the PDE combustor to a certain level at which time the next cycle can be started. The effect of the nozzle geometry on the cycle time needs to be investigated. Therefore, it is important to systematically investigate the effects of the geometry of the nozzle on the PDE performance.

In this section, the effect of attaching a nozzle with a PDE tube is discussed. In the following sections, the results of a systematic study to investigate the effects of different nozzle geometries are presented.

Here the reference configuration is a simple cylindrical PDE tube of constant cross-section without any external nozzle. The PDE tube, 30 cm in length and 4 cm in diameter, is uniformly filled with stoichiometric hydrogen-air mixture. Both ambient pressure and the initial fill pressure are chosen to be 1 atm. Initial temperature of the PDE chamber is 300 K. Detonation initiation is assured by having a large amount of energy deposition near the closed-end (thrust wall) of the tube. This is achieved by creating a high pressure and high temperature region near the closed-end. Temperature and pressure in this region are set at 1500 K and 10 atm respectively. Computations were performed for a single pulse in a two-dimensional-axisymmetric configuration. Three basic nozzle configurations were investigated: straight nozzle, diverging nozzle, and converging nozzle.

Diverging Nozzle

This section examines the effects of adding a divergent nozzle with a PDE tube. Here the reference PDE tube is compared with the configuration where a diverging nozzle, 15 cm in length with an exit radius of 3.5 cm, is added at the aft end of the PDE tube. Figure 23 shows a schematic of the computed configuration where a divergent nozzle is connected at the open-end of the PDE tube. During the computations, the total thrust of the engine (the integrated wall pressure) is monitored. The results are shown in Figure 24. The high initial peak value of thrust is due to the large amount of energy deposition near the closed-end of the PDE tube for detonation initiation. The amount of impulse from the detonation initiation process can be estimated by running the computation without chemical reactions (i.e. without

detonation initiation). From the thrust profile it can be observed that up to approximately 1.5 ms thrust profile is same for the reference case and for the divergent nozzle case. This period refers to traveling of the detonation wave through the PDE tube. For the divergent nozzle case, the detonation wave enters the nozzle section at around 1.5 ms. The thrust level then starts to increase sharply attaining a maximum value (the second peak of the thrust profile) at 3 ms when the detonation wave reaches the nozzle exit. This period (from 1.5 ms to 3 ms) refers to traveling of the detonation wave through the nozzle section. The thrust then decreases as the detonation wave leaves the nozzle and takes on negative values when the average pressure inside the PDE tube drops below the ambient pressure.

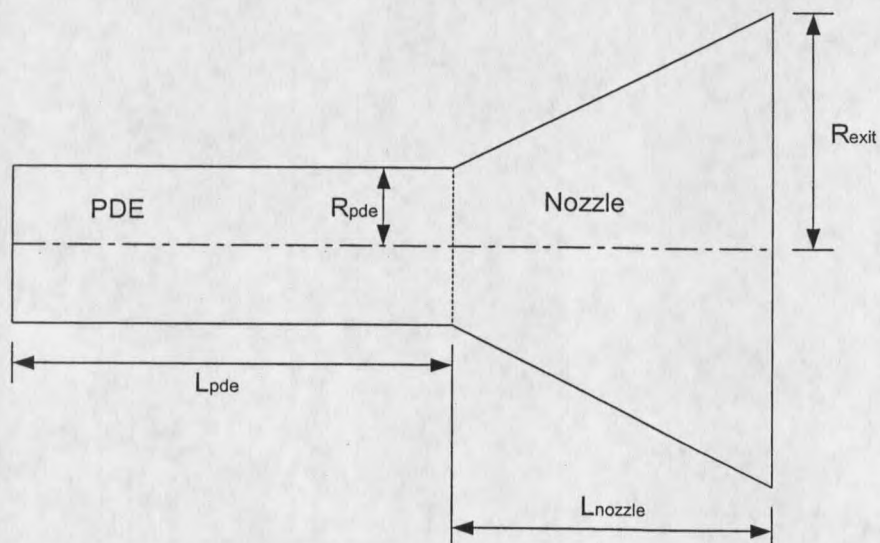


Figure 23. Schematic of a divergent nozzle attached with a PDE tube

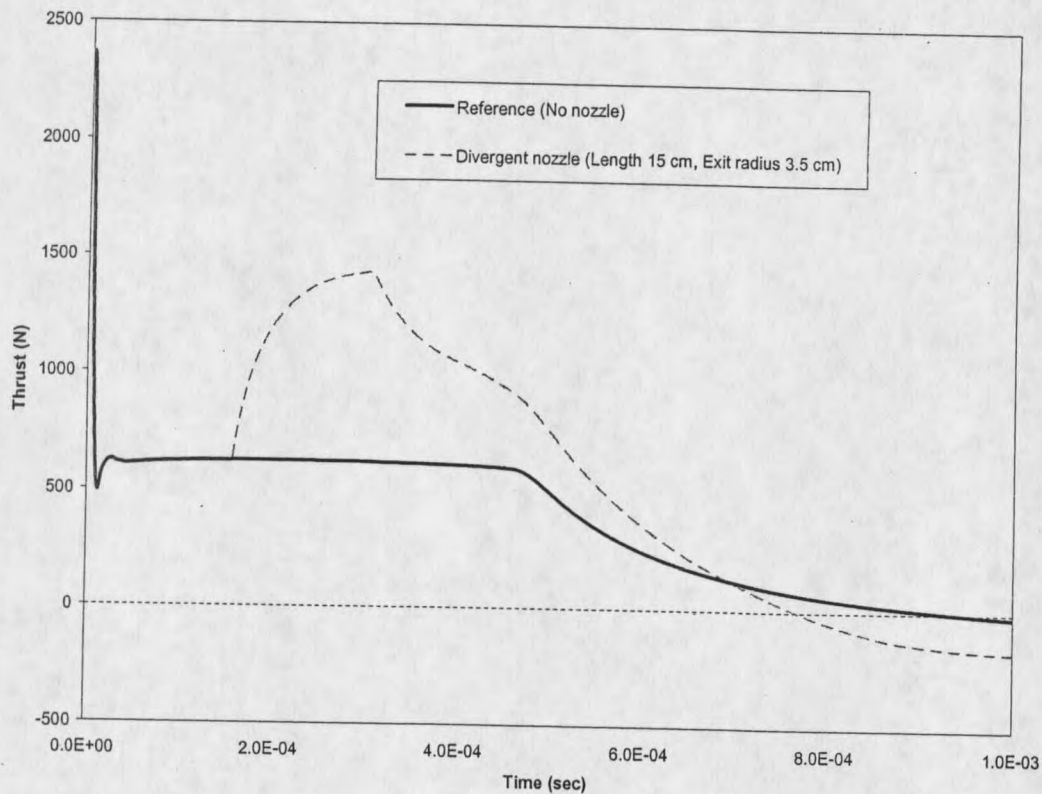


Figure 24. Effect of divergent nozzle on the thrust

Figure 25 shows the total impulse (force integrated over time) as a function of time. The results show that the addition of a divergent nozzle is marked by a significant increase in the total impulse generation. The attachment of the diverging nozzle with the PDE tube leads to about 51.8% increase in the maximum impulse. From Figure 25 rapid impulse generation can be observed for the diverging nozzle case than the reference case, which indicates that the presence of diverging nozzle enhances the impulse generation rate.

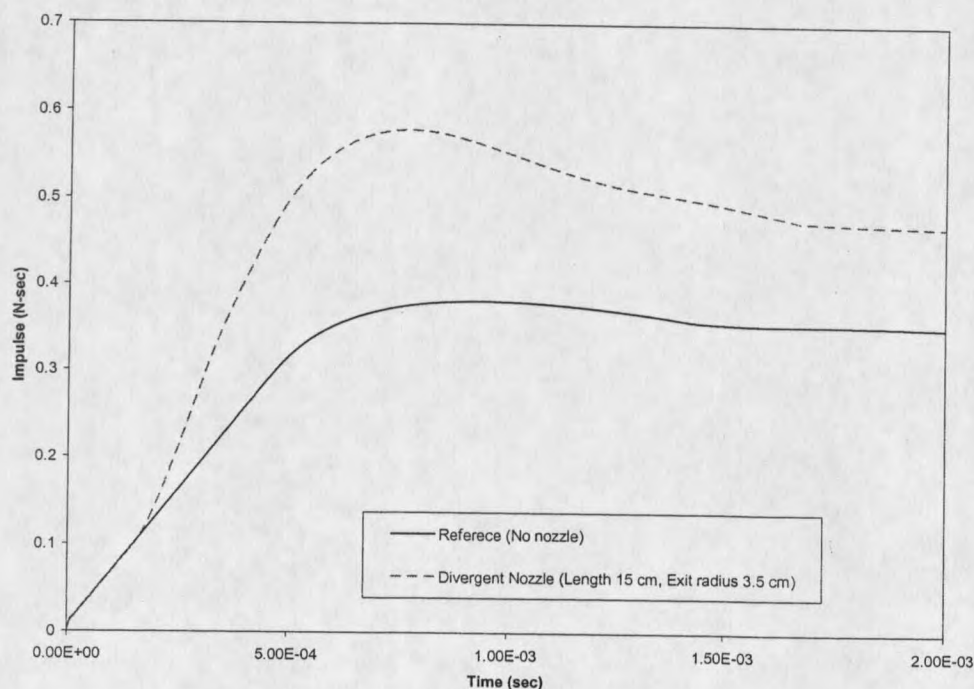


Figure 25. Effect of divergent nozzle on the impulse

The impact of adding a diverging nozzle with a PDE tube appears attractive. A diverging nozzle increases the effective thrust wall area. Therefore, the addition of a diverging nozzle results in more impulse generation. Following Cooper et al. (2000), the presence of a divergent nozzle with a PDE tube delays the arrival of expansion waves inside the tube from the exit and prolongs the thrust generation. For a better understanding one may first consider the case where no nozzle is attached with the PDE tube. In this case, the detonation wave, initiated at the closed-end of the PDE tube, travels through the propellant mixture towards the open-end and reaches the tube exit. The detonation wave causes an enormous rise in temperature and pressure of the propellant mixture inside the PDE tube. As the pressure outside the tube is ambient, a pressure differential exists at the open-end of the tube. When the

detonation wave leaves the tube, expansion waves are generated at the tube exit due to the pressure differential. These expansion waves proceed toward the closed-end of the tube causing pressure drops inside the tube. Now adding a divergent nozzle delays the arrival of the expansion waves inside the PDE tube, increasing the pressure relaxation time. The pressure histories of the reference case and the divergent nozzle case (Figure 26) confirm this explanation. As shown in Figure 26, for the reference case the pressure drops to 1 atm at around 0.9 ms, whereas for the divergent nozzle case this time is 1 ms, which is 11% higher than the previous value. Therefore, the gas resides inside the PDE tube for a longer time resulting in prolonged thrust production and more impulse generation.

Figure 27 shows the PDE temperature as a function of time for the reference case and the divergent nozzle case. As shown in this figure, when the divergent nozzle is present the temperature inside the PDE tube drops at a slower rate than the reference (no nozzle) case, which is due to the delay in the arrival of expansion waves as mentioned above. In this section only one divergent nozzle geometry was examined. More investigations on different divergent nozzle geometries are discussed later.

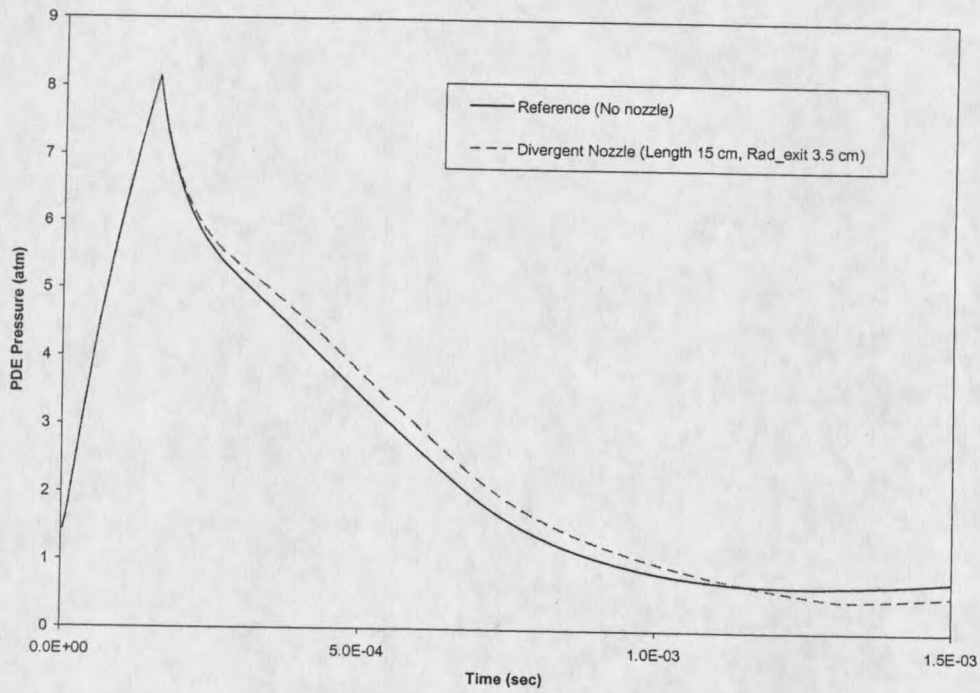


Figure 26. Effect of divergent nozzle on PDE pressure history

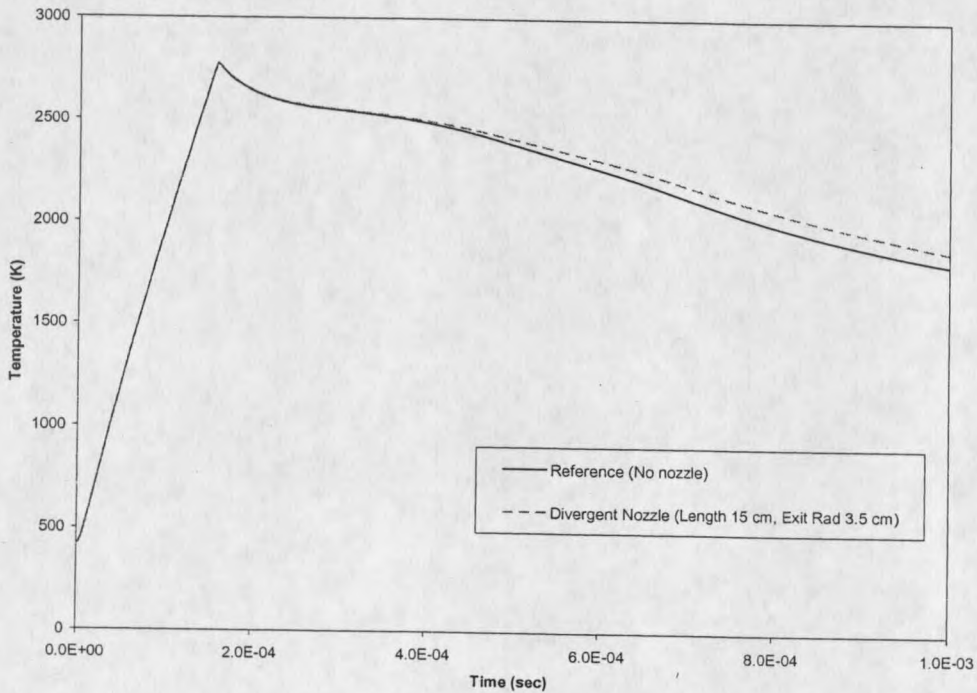


Figure 27. Effect of divergent nozzle on PDE temperature

Straight Nozzle

This section investigates the effects of adding a straight nozzle with a PDE tube. The reference no nozzle case is compared with the configuration where a straight nozzle is connected at the open end of the PDE tube. Here, the diameter of the straight nozzle is the same as the diameter of the PDE tube. Two different straight nozzle geometries are considered: in the first configuration the nozzle is 10 cm long and in the second configuration the nozzle is 30 cm long.

Figures 28 and 29 show the total thrust and the total impulse as functions of time. It is evident from the results that the addition of a straight nozzle prolongs the thrust generation and increases the total impulse. A closer look at the thrust profile reveals that for the reference case, a positive thrust is generated until approximately 0.9 ms; whereas for the straight nozzle case this time is approximately 1.8 ms. This indicates an increase in the thrust generation time in the presence of a straight nozzle. From the impulse profile it can be seen that when a 10 cm long straight nozzle is attached there is about 23% increase in the maximum impulse. The configuration with the 30 cm long nozzle produces more impulse as it results in about 55% increase in the maximum impulse. The higher impulse generation due to the attachment of a straight nozzle can be explained in a similar way as the effects of a divergent nozzle were discussed in the previous section. The presence of a straight nozzle section at the end of the PDE tube delays the arrival of expansion waves from the exit increasing the pressure relaxation time. The pressure histories for the different configurations (Figure 30) confirm this explanation originally given by Cooper et al.

(2000). As discussed earlier, when a nozzle is connected with the PDE tube the gas resides inside the tube for longer times due to the delayed arrival of expansion waves. This in turn results in prolonged thrust and more impulse generation.

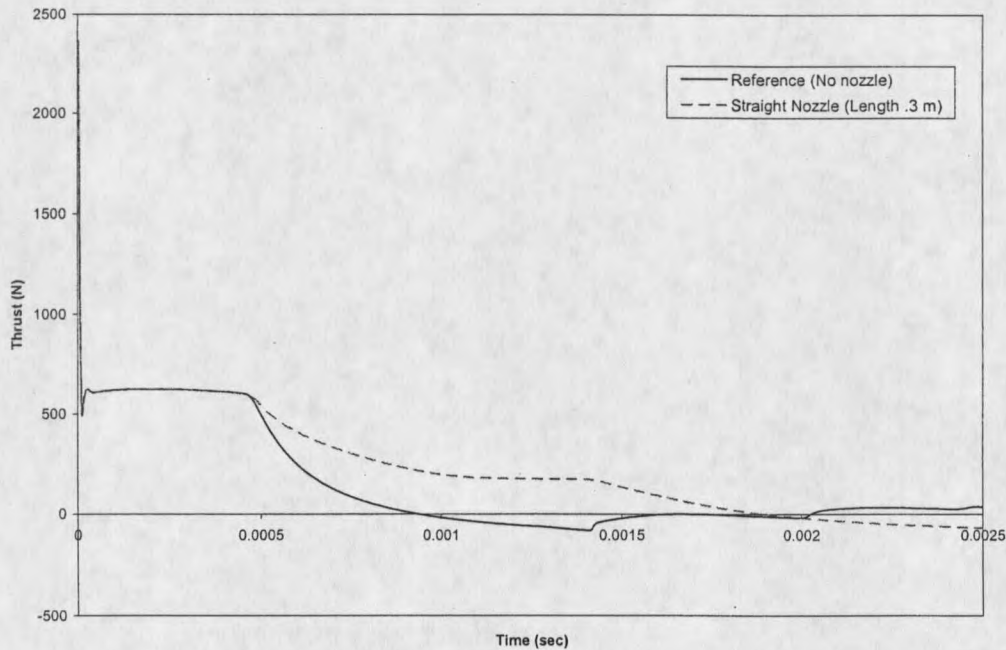


Figure 28. Effect of straight nozzle on the thrust

The above-discussed results suggest that addition of a straight nozzle is very effective in increasing the total impulse generation. However, it can be noted that with a straight nozzle, the maximum impulse was obtained at a time later than the reference case. As indicated in Figure 29, the arrival time of maximum impulse with the 30 cm long nozzle is approximately twice than that required for the reference configuration. For the reference configuration the maximum impulse was obtained at

approximately 0.75 ms. Whereas for the 10 cm long nozzle it was produced at around 1 ms, and for the 30 cm long nozzle the time was approximately 2 ms.

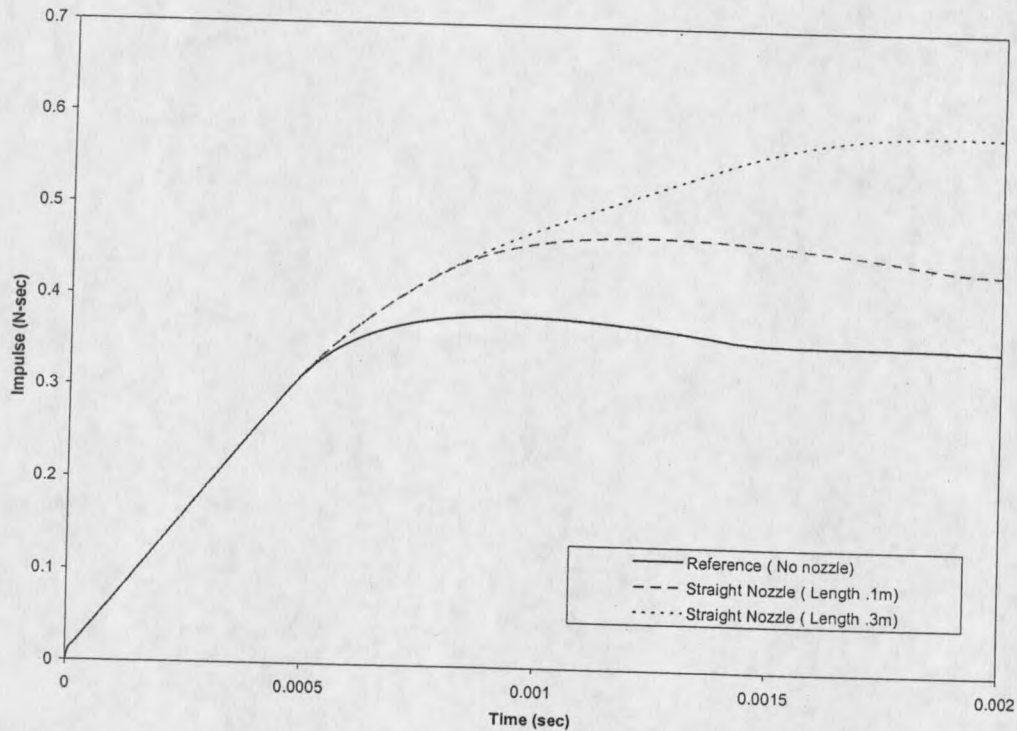


Figure 29. Effect of straight nozzle on the impulse

The results of the performed investigations suggest that both the diverging and straight nozzle effectively increase the impulse generation of a PDE. It would be interesting to compare the performance gains using a straight nozzle and a divergent nozzle of the same length. It was observed that the addition of a 30 cm long straight nozzle with the PDE tube increased the maximum impulse by 55%. In contrast, the addition of a diverging nozzle of the same length (with an exit of radius 4 cm) results in about 60% increase in impulse generation. Therefore, the addition of a divergent

nozzle looks potentially attractive. More investigations on different straight and divergent nozzle geometries are discussed later.

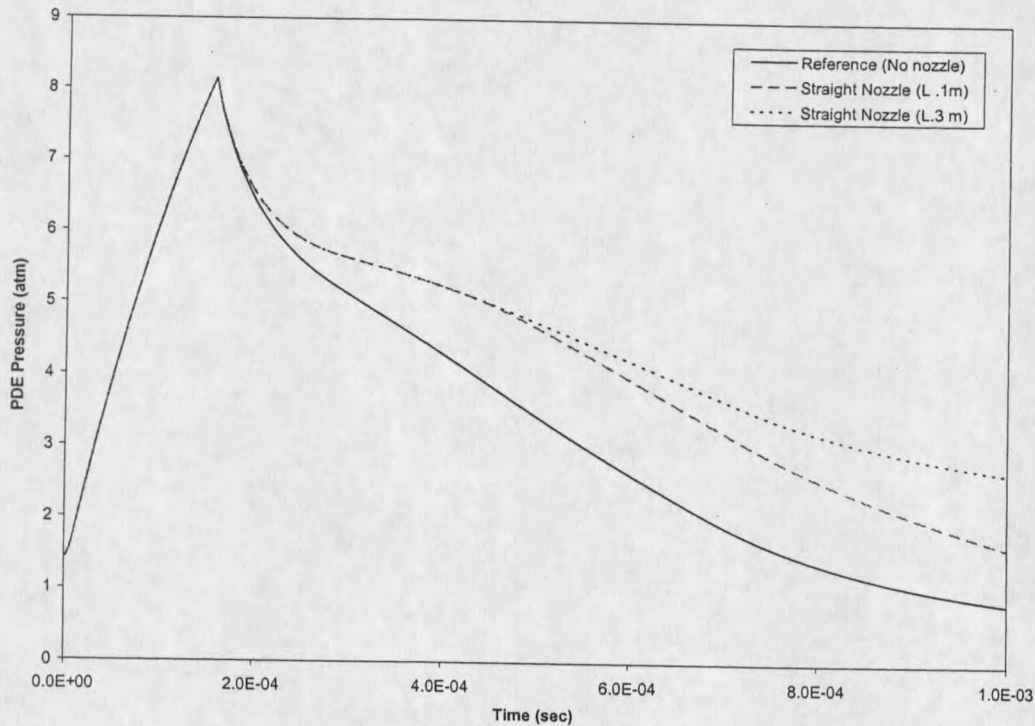


Figure 30. Effect of straight nozzle on PDE pressure history

Converging Nozzle

In order to investigate the effect of nozzle addition with a PDE tube, numerical studies were performed for different convergent nozzle geometries. Here, the reference PDE tube is compared to the configurations where a converging nozzle is connected to the open end of the PDE tube. Figure 31 shows a schematic of the computed configurations. Two different conical converging nozzle shapes were considered in this investigation. In the first configuration (Shape 1) the nozzle section

is 10 cm long with an exit radius of 1.5 cm, and in the second configuration (Shape 2) the nozzle is 30 cm long with an exit radius of 1.5 cm. The different configurations can be listed as below,

Shape 1: $L_{\text{nozzle}} = 10 \text{ cm}$, $R_{\text{exit}} = 1.5 \text{ cm}$

Shape 2: $L_{\text{nozzle}} = 30 \text{ cm}$, $R_{\text{exit}} = 1.5 \text{ cm}$

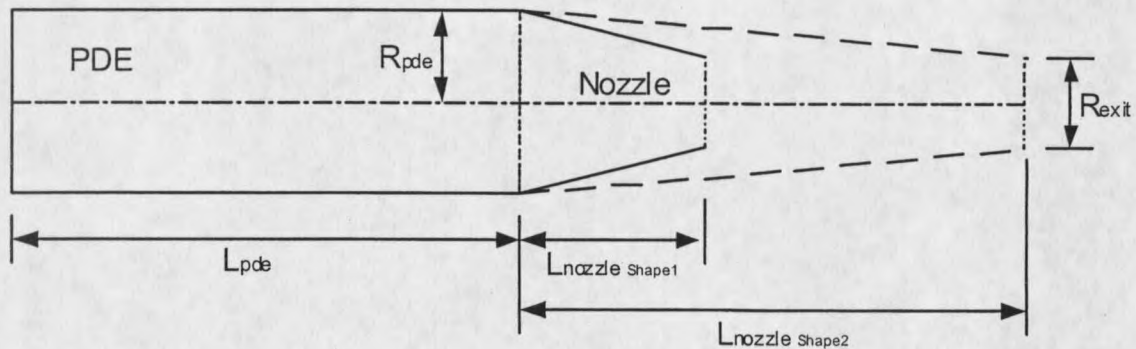


Figure 31. Schematic of the computed configuration for PDE tube with convergent nozzles of different shapes

Figure 32 illustrates the effect of attachment of a convergent nozzle on the generated impulse. Here the total impulse is shown as a function of time. It can be observed that a higher impulse is generated in the presence of a converging nozzle. The addition of the shorter converging nozzle (Shape1) leads to about 15% increase in the maximum impulse. The other configuration (Shape 2) leads to about 27% increase in the maximum impulse. One noticeable observation is that between the two different geometries, the longer nozzle (Shape 2) produces the larger impulse. A close observation of the impulse trace reveals that the addition of a converging nozzle leads

